

SOVIET PHYSICS USPEKHI

A Translation of Uspekhi Fizicheskikh Nauk

SOVIET PHYSICS USPEKHI

(Russian Vol. 81. Nos. 3-4)

MAY-JUNE 1964

PROBE METHODS IN PLASMA RESEARCH

Yu. M. KAGAN and V. I. PEREL'

Usp. Fiz. Nauk 81, 409-452 (December, 1963)

CONTENTS

I. Electron part of probe characteristic with negative probe potential	768
II. Ion part of probe characteristic with negative probe potential	770
III. The method of two probes	777
IV. Use of the probe method under more complicated conditions	781
V. Improvement of probe measurement techniques and errors of the method	785
List of symbols	791
Cited literature	791

1. Introduction

THE probe method is one of the main methods of determining plasma parameters. This review is devoted to an exposition of the contemporary status of the probe techniques.

In the attempt to relate the properties of a plasma with the elementary processes that occur in it calls for knowledge of such parameters as the electron concentration n_0 and the electron velocity distribution $f_0(v)$ at a given point of the plasma. The probe method, proposed by Langmuir in 1923, consists of placing an electric probe, that is, a small spherical, cylindrical, or plane electrode at a given location in the discharge, and making the probe potential lower or higher than the plasma potential u_0 at this point. If the probe potential differs from u_0 , then an electric field is produced in its surrounding space, accelerating charges of one sign and repelling charges of the opposite sign. In practice, probe measurements are made with the circuit shown in Fig. 1. The probe is kept at varying potentials relative to the cathode or the anode. The total probe current i consists of the ion current i_p and the electron current i_e .

The probe characteristic is the dependence of the total probe current on the probe potential. Its general form is shown in Fig. 2. The characteristic can be qualitatively interpreted in the following manner: at a large negative probe potential the entire probe current is due to the positive ions (Section AB). When the negative potential is decreased an electron current due

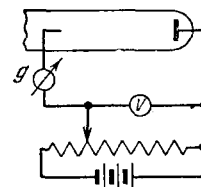


FIG. 1. Probe measurement circuit.

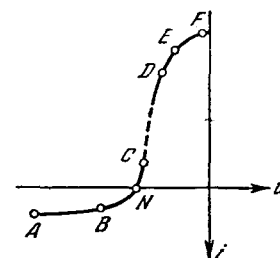


FIG. 2. General view of probe characteristic.

to the fast electrons that pass through the retarding field at the probe is superimposed on the ion current. This superposition explains the rapid decrease of the current and the subsequent reversal of its sign at potentials that are even lower than the space potential* (Section BC). With decreasing negative probe potential, the current increases rapidly, owing to the decrease in the retarding field at the probe. Even in this region (CD) the electron current greatly exceeds the ion current. When the field retarding the electrons disappears and turns into an accelerating field, the law governing

*The space potential is called the potential of that part of the plasma in which the probe is situated.

the increase of the electron current changes, and this is manifest in a more or less sharp break in the characteristic near the space potential (Section DE).

In order to find the plasma parameters, it is necessary to calculate the type of probe characteristic, using some simplified theoretical scheme, and to compare it with the observed characteristic. The electron part is employed (region CE of Fig. 2) in the overwhelming majority of investigations. This is connected with the simplicity of the theory^[1,2] for this part of the characteristic. There are many cases of practical importance, however, in which the use of the electron part is impossible or difficult. These include: (1) discharges at large current densities, when it is difficult to obtain the entire region CE, because of overheating of the probe or because of the jumping of the discharge over to the probe; (2) discharges in a magnetic field, when the electron part is greatly distorted; (3) electrodeless discharges. In such cases it is convenient to employ the ion part of the characteristic AC of Fig. 2. The advantages lie in the fact that the current flowing in the probe is not large. The magnetic field influences less this part of the characteristic, since both ions and fast electrons move to the probe. Finally, in the two-probe method, the ion part can be reproduced almost completely.

The theory of the ion part of the characteristic was first presented by Langmuir and Mott-Smith^[1,2]. The theory was based on separating the plasma around the probe into a quasineutral plasma and a space-charge sheath, and assuming that there is no field at all in the quasineutral plasma. This theory turned out to be incorrect. Since the ion energy in the discharge is much smaller than the electron energy, even a weak field penetrating into the quasineutral region greatly distorts the motion of the ions. This field causes the ions to be gathered not by the surface of the probe or of the sheath, but by a large-radius surface lying in the quasineutral region. A correct theory of the ion saturation current with a negative probe potential was first presented by Bohm, Burhop, and Massey^[3] and developed further by others^[4-11].

Attempts were made to determine the plasma parameters from the electron saturation region EF (Fig. 2). However, the form of this part of the characteristic is greatly influenced by reflections. These attempts therefore were not continued. The electron saturation region will not be considered in the present review.

The properties of the plasma near the probe are modified by the presence of the probe. However, at sufficiently large distances from the probe the plasma remains practically unperturbed. In the present review we consider the conditions under which the pressure of the gas is sufficiently small, so that this distance (an estimate of which will be presented below) is much smaller than the mean free paths of the electrons and ions. Then the collisions do not exert any

influence on the motion of the particles in the perturbed region.

At such pressures we can therefore disregard collisions completely when calculating the probe current.

In Ch. I-III we assume the unperturbed plasma to be homogeneous, isotropic, and consisting of only electrons and positive ions of one sort. Cases when these conditions are violated are considered in Ch. IV.

I. ELECTRON PART OF PROBE CHARACTERISTIC WITH NEGATIVE PROBE POTENTIAL

2. Theory

According to the Liouville theorem, the electron distribution function does not change along the particle trajectory in the space \mathbf{r}, \mathbf{v} . Therefore

$$f(\mathbf{r}, \mathbf{v}) = f(\mathbf{r}_0, \mathbf{v}_0), \quad (1)$$

where \mathbf{r} and \mathbf{v} are the coordinate and velocity of the particle, which has at the initial instant a coordinate \mathbf{r}_0 and a velocity \mathbf{v}_0 . We shall assume that the electron distribution in the unperturbed region is isotropic and homogeneous, so that the distribution function depends only on the energy

$$f(\mathbf{r}_0, \mathbf{v}_0) = n_0 f_0 \left(\frac{mv_0^2}{2} \right).$$

Then according to (1) and the energy conservation law

$$\frac{mv_0^2}{2} = \frac{mv^2}{2} + eV(\mathbf{r})$$

we get

$$f(\mathbf{r}, \mathbf{v}) = n_0 f_0 \left[\frac{mv^2}{2} + eV(\mathbf{r}) \right]. \quad (2)$$

$f(\mathbf{r}, \mathbf{v})$ will be determined by formula (2) only for those values of \mathbf{r} and \mathbf{v} which the electron can attain as it moves from the unperturbed region without crossing the probe surface. At values of \mathbf{r} and \mathbf{v} for which this is impossible, $f(\mathbf{r}, \mathbf{v})$ will be distorted; in particular, $f(\mathbf{r}, \mathbf{v}) = 0$ for these values in the case of a completely absorbing probe. The region of these values of \mathbf{r} and \mathbf{v} will be called the region screened by the probe. To find the limits of the screened region it is necessary, generally speaking, to know the variation of the potential $-V(\mathbf{r})$ and to solve completely the problem of mechanical motion of the electron in this field. To determine whether the phase-space point \mathbf{r}, \mathbf{v} is situated in the screened region or not it is necessary to trace the particle trajectory before it reaches this point. If this preceding trajectory goes from the unperturbed region to the point \mathbf{r} without crossing the probe, then the point \mathbf{r}, \mathbf{v} belongs to the unscreened region. If the surface of the probe is convex, the boundaries of the screened region on the probe surface can be readily obtained. It is obvious that at each point of the probe surface the distribution of the electrons that have velocities directed towards the probe will not be distorted by the probe surface. The distribution of electrons

with velocities directed away from the probe is distorted. In other words, if ϑ is the angle between the electron velocity vector on the probe surface and the inward normal to the surface, then the distribution function on the surface $f(a, \mathbf{v})$ is determined by formula (2) in which we must replace $-V(\mathbf{r})$ by the probe potential $-V$ for $\vartheta < \pi/2$; the distribution function is distorted when $\vartheta > \pi/2$, and is in particular equal to zero in the case of an absorbing probe. (If the surface of the probe were not convex, then the part of the region with $\vartheta < \pi/2$ would also be screened.) Thus, the electron distribution function at the probe surface does not depend on the variation of the potential between the probe and the unperturbed plasma, but depends on the probe potential. The same pertains to the electron current density in the probe, which is determined by the following expression (in the case of an absorbing probe)

$$j_e = 2\pi e \int_0^{\pi/2} \sin \vartheta d\vartheta \int_0^\infty v \cos \vartheta f(a, \mathbf{v}) v^2 dv$$

$$= \pi e n_0 \int_0^\infty v^3 f_0 \left(\frac{mv^2}{2} + eV \right) dv,$$

or

$$j_e = \frac{2\pi e n_0}{m^2} \int_{eV}^\infty (e - eV) f_0(\epsilon) d\epsilon. \tag{3}$$

We note that the density of the electron current does not depend in this case on the form of the probe, if the probe surface is convex. Differentiating (3) twice with respect to V , we obtain

$$\frac{d^2}{dV^2} j_e = \frac{2\pi e^3}{m^2} n_0 f_0(eV). \tag{4}$$

This formula*, which makes it possible to determine the electron velocity distribution function in the unperturbed region from the second derivative of the electron current in the probe, was first used by Druyvestein^[12]. Methods of experimental determination of the second derivative of the electron current will be detailed later (Sec. 27). If the electrons have in the unperturbed region a Maxwellian distribution, that is,

$$f_0(\epsilon) = \left(\frac{m}{2\pi k T_e} \right)^{3/2} \exp \left(-\frac{\epsilon}{k T_e} \right),$$

then

$$j_e = \frac{n_0 e \bar{v}_e}{4} \exp \left(-\frac{eV}{k T_e} \right). \tag{5}$$

Formula (5) was first derived by Langmuir and is

*If we introduce in place of $f_0(\epsilon)$ an energy distribution function $f'_0(\epsilon)$ with the aid of the relation

$$f'_0(\epsilon) d\epsilon = 4\pi v^2 f_0(\epsilon) dv,$$

then

$$n_0 f'_0(eV) = \frac{2\sqrt{2}}{e^2} \sqrt{\frac{m}{e}} \sqrt{V} \frac{d^2}{dV^2} j_e. \tag{4a}$$

widely used in plasma research. The form of the probe characteristic for the case when the electron velocities have a Druyvestein distribution was calculated in ^[13].

We note in conclusion that in the presence of elastic reflection of the electrons from the probe

$$j_e = 2\pi e n_0 \int_0^{\pi/2} \cos \vartheta \sin \vartheta d\vartheta \int_0^\infty v^3 [1 - \alpha(v, \vartheta)] f_0 \left(\frac{mv^2}{2} + eV \right) dv,$$

where $\alpha(v, \vartheta)$ — reflection coefficient. If f_0 is a Maxwellian function, then the expression for the probe current density will differ from (5) only by a factor $(1 - \overline{\alpha v_e} / \bar{v}_e)$, which does not depend on the probe potential (the bar denotes averaging over the Maxwellian distribution), so that reflection does not influence the determination of the temperature T_e . Data on the electron reflection coefficient are given for several surfaces, for example, in ^[14].

3. Simplest Method of Processing the Characteristic

The total probe current on section CDEF (Fig. 2) is practically all due to the electrons, and consequently the characteristic is described by Eq. (3). The presence of a linear section in region CD on a semilog plot of i vs. u , as in Fig. 3., is evidence that the electron velocity distribution is Maxwellian [see (5)]. The temperature of this distribution can then be determined from the slope of the linear section, using the relation

$$T_e = \frac{e}{k} \frac{du}{d \ln |i|} = \frac{e}{k} \frac{1}{\operatorname{tg} \psi} \tag{6}^*$$

(ψ — angle between the linear section and the abscissa axis).

The location of the break in the semilog characteristic determines the space potential u_0 . The current corresponding to the space potential makes it possible to find the electron concentration in the unperturbed plasma [see (5) with $V = 0$]

$$n_0 = \frac{4i_0}{e v_e S}. \tag{7}$$

In fact, the break in the characteristic is not abrupt. Strictly speaking, the space potential corresponds to the start of the deviation of the characteristic from linearity. However, the concentration determined from the current at this point is overestimated because of the reflection of the electrons from the probe. The magnitude of this reflection cannot be readily estimated, since the state of the probe surface is unknown.

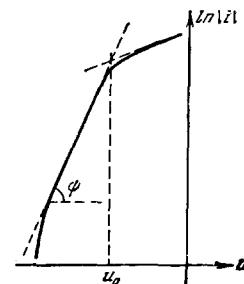


FIG. 3. Electron part of probe characteristic in a semilog plot. The deviation from linearity of the lower part of the curve is due to the presence of the ion current.

* $\operatorname{tg} = \tan$.

Langmuir proposed a method for determining the space potential from the point of intersection of sections CD and EF (Fig. 3). One can hope that in this method account is taken, to some degree, of the influence of reflection on the magnitude of the current at the space potential, since the reflections have a smaller effect on section EF, corresponding to the motion of the electrons in the attracting field of the probe. On the other hand, comparison of the electron concentrations in a low-pressure mercury discharge, obtained by the probe and microwave methods, shows in this case a somewhat better agreement when the space potential is determined from the deviation of the characteristic from linearity [15].

4. Elimination of the Influence of the Ion Current

In order to eliminate the ion current in those parts of the characteristic where it is comparable with the electron current (section BC of Fig. 2), it is advisable to use the first derivative of the probe current with respect to the potential [8]. The electron component could be separated from the total current by extrapolating the ion part from Sec. AB of Fig. 2. However, as will be shown later, the law governing such extrapolation is not known accurately, and the extrapolation errors can greatly influence the value of the electron current in the region BC. Since the ion current changes much more slowly than the electron current in region BC (the ions move in an attracting field, while the electrons move in a retarding field), we get

$$\frac{di}{du} \approx -\frac{di_e}{du}.$$

For a Maxwellian distribution the plot of $\ln(di_e/du)$ against u is a straight line, the slope of which determines T_e . This method of determining T_e is important when the region of the characteristic CD is distorted or cannot be obtained (see Sec. 1).

II. ION PART OF PROBE CHARACTERISTIC WITH NEGATIVE PROBE POTENTIAL

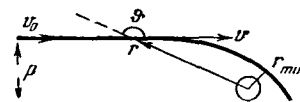
5. Concept of Limited Motion

At large negative probe potentials in region AB, the total probe current is practically equal to the ion current. Therefore, to use this part of the characteristic it is necessary to develop a theory for the ion current in a probe that attracts ions. We shall examine the characteristic features of the motion in an attracting field with a spherical probe as an example. In this case the energy and momentum conservation laws apply:

$$\left. \begin{aligned} \frac{Mv_0^2}{2} &= \frac{Mv^2}{2} - eV(r), \\ pv_0 &= rv \sin \vartheta, \end{aligned} \right\} \quad (8)$$

where p — impact parameter, v_0 — velocity of the ion away from the probe, ϑ — angle between the radius

FIG. 4. Motion of ion in the attracting field of the probe.



vector and the direction of the velocity at the point r (Fig. 4).

When the ion is at the minimum distance $r = r_m$ from the probe, we have $\sin \vartheta = 1$. From (8) we obtain the connection between the impact parameter and the minimum distance between the ion and the probe:

$$p^2 \equiv G(r_m) = r_m^2 \left[1 + \frac{2e}{Mv_0^2} V(r_m) \right]. \quad (9)$$

In the case of repulsion, $eV(r) < 0$ and $G(r_m)$ is a monotonically increasing function of r_m . Therefore for each value of the impact parameter there will exist a minimum distance from the particle to the probe. The particles reaching the probe are those for which $p^2 \leq G(a)$. In the case of attraction $eV(r) > 0$ and the function $G(r_m)$ is a product of two factors, of which one increases with distance from the probe and the other decreases. Two possibilities exist in this case:

a) $G(r_m)$ is a monotonic increasing function of r_m (Fig. 5a). Then, as in the case of repulsion, the particles for which $p^2 \leq G(a)$ will reach the probe.

b) $G(r_m)$ is a nonmonotonic function of r_m . Let the smallest value of this function be attained at the point r_l , which generally speaking depends on v_0 (Fig. 5, curve b). Then the impact parameters which satisfy the condition $p^2 \leq G(r_l)$ will not correspond to any minimum distance, that is, particles with such impact parameters will strike the probe.* If $r_l > a$, then the role of the gathering surface will be assumed not by the surface of the probe, but by a sphere of radius r_l . We shall call this the case of limitation motion. As will be shown later, this is precisely the case which is realized when an ion moves in the attracting field of the probe.

In the case of a cylindrical probe, all the formulas and derivations of this section remain valid if we define v_0 or v as the projections of the velocity on a plane perpendicular to the probe axis, and define r and p as the corresponding distances in this plane.

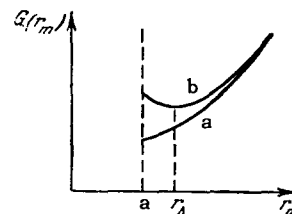


FIG. 5. Plot of $G(r_m)$: a) in the absence of limitation motion; b) in the presence of limitation motion.

*When $p^2 > G(r_l)$ the minimum distance is determined by the root of (9) corresponding to the section on which $G(r)$ increases. In fact, when $r = r_m$ the radial velocity component is $\dot{r} = 0$. It is furthermore easy to show that $\ddot{r} = (v_0^2/2r_m^2) dG/dr$ when $r = r_m$, so that $\ddot{r} > 0$ on the section where the function G increases.

6. Simplified Theory of Ion Part of the Characteristic

Formulas for the ion current on the surface of the sheath can be obtained by starting from simple physical considerations^[3,6]. The presence of limited motion signifies that outside the sheath, in the quasineutral region, there is a surface such that an ion reaching it strikes the probe. Consequently, the ions strike the surface of the sheath almost radially. The potential on the surface of the layer V_S should be of the order of kT_e , since the sheath begins where the electron concentration begins to drop noticeably. If the ion temperature is smaller than the electron temperature, then the velocity of the ion on the boundary of the sheath is $(2eV_S/M)^{1/2}$. The concentration of the ions at the external boundary of the sheath is determined from the condition of quasineutrality by the expression $n_0 \exp(-eV_S/kT_e)$.* We thus have for the ion current in the probe

$$i_p = en_0 e^{-\frac{eV_S}{kT_e}} \sqrt{\frac{2eV_S}{M}} S_S, \tag{10}$$

where S_S — area of the sheath surface. Expression (10) is not very sensitive to the choice of the value of S_S , if it is of the order of kT_e . We then obtain

$$i_p = cn_0 e \sqrt{\frac{2kT_e}{M}} S_S, \tag{11}$$

where c — a coefficient of the order of unity, which coincides with the formulas obtained below for the spherical ($c = 0.8$) and cylindrical ($c = 0.4$) cases. The foregoing instructive derivation enables us to apply formula (11) to probes of different shapes, for example to a finite plane probe, the rigorous calculation for which is difficult. The surface area of the sheath S_S can be chosen in practice equal to the area of the probe surface. In fact, S_S increases somewhat with the increasing of the potential, and therefore the ion part of the characteristic does not have a strict saturation.

A. SPHERICAL PROBE

7. General Expression for Ion Current

We consider ions which have away from the probe velocities in the interval d^3v_0 . The flux of such particles to the probe is equal to the flux through the area $\pi p_0^2 = \pi G(r_l)$ (p_0 — maximum impact parameter, at which the ion reaches the probe), that is, equal to $n_0 \pi G(r_l) F_0(v_0) v_0 d^3v_0$. The total current is obtained by integrating this expression with respect to the initial velocities:

$$i_p = 4\pi^2 en_0 \int_0^\infty G(r_l) F_0(v_0) v_0^3 dv_0. \tag{12}$$

In the absence of limiting motion, the gathering sur-

face is the probe surface and $r_l = a$. Then

$$G(r_l) = G(a) = a^2 \left[1 + \frac{2e}{Mv_0^2} V(a) \right]$$

and for a Maxwellian distribution

$$i_p = \frac{4\pi a^2 \bar{v}_p n_0}{4} \left(1 + \frac{eV}{kT_p} \right). \tag{13}$$

In view of the fact that the limiting motion actually does take place (see below), formula (13) is not correct. However, for a real calculation of the current by means of formula (12) it is necessary to know the variation of the potential in the vicinity of the probe, which should determine also the dependence of r_l on v_0 . Expression (12) can be simplified by replacing the real ion distribution over the velocities in the unperturbed plasma by a distribution in which all the ions have identical energy ϵ_0 , that is, by putting

$$F_0(v_0) v_0 = \frac{M}{4\pi} \delta \left(\frac{Mv_0^2}{2} - \epsilon_0 \right). \tag{14}$$

Such a substitution is valid because the ions are in an accelerating field. There is a certain vagueness in the definition of ϵ_0 , which should be equal to the average ion energy in the unperturbed plasma, accurate to a factor of the order of unity. As will be shown below, the ion current in the probe is practically independent of ϵ_0 if $T_p < T_e$. With the aid of (12) and (14) we get

$$i_p = \frac{4\pi r_l^2 en_0 v_p}{4} \left[1 + \frac{eV(r_l)}{\epsilon_0} \right], \quad \frac{Mv_p^2}{2} = \epsilon_0. \tag{15}$$

Formula (15) differs from (13) in that the role of the probe radius is assumed by the role of the limitation sphere.

8. Connection Between the Ion Concentration in the Vicinity of the Probe and the Potential Distribution

Let us find the concentration of the ions in the vicinity of the probe that attracts them. To this end it is necessary, in accordance with Sec. 2, to obtain the limits of the screening region. We shall assume that the function $G(r)$ has the form shown in Fig. 5b.

The phase-space point \mathbf{r}, \mathbf{v} belongs to the unscreened region, if the ion reaches it from the unperturbed plasma. To this end it is first necessary to satisfy the condition

$$\frac{Mv_0^2}{2} = \frac{Mv^2}{2} - eV(r) > 0. \tag{16}$$

When $r > r_l$, the point \mathbf{r}, \mathbf{v} will belong to the unscreened region if $\vartheta > \pi/2$, or else if $\vartheta < \pi/2$ but $p^2 > G(r_l)$. According to the conservation laws (8), the last condition can be rewritten in the form

$$\vartheta > \vartheta_1,$$

where

$$\sin^2 \vartheta_1 = \frac{v_0^2 G(r_l)}{v^2 r^2}, \quad \vartheta_1 < \frac{\pi}{2}. \tag{17}$$

The ion can arrive at the point $r < r_l$ from the unper-

*We assume approximately that the electrons have a Boltzmann distribution in the repelling field of the probe.

turbed region if $\vartheta > \pi/2$ and $p^2 < G(r_l)$, that is, if $\vartheta > \vartheta_l$, where

$$\sin^2 \vartheta_2 = \frac{v_0^2 G(r_l)}{v^2 r^2}, \quad \vartheta_2 > \frac{\pi}{2}. \quad (18)$$

The ion concentration at a distance r from the probe can thus be written in the form

$$n_p = 2\pi \int_{\sqrt{-\frac{2eV}{M}}}^{\infty} n_0 F_0 \left[\frac{Mv^2}{2} - eV(r) \right] v^2 dv \psi(v, r),$$

where

$$\left. \begin{aligned} \psi(v, r) &= \int_{\vartheta_1}^{\pi} \sin \vartheta d\vartheta \quad r > r_l, \\ \psi(v, r) &= \int_{\vartheta_2}^{\pi} \sin \vartheta d\vartheta \quad r < r_l. \end{aligned} \right\} \quad (19)$$

Calculation of the concentration $n_p(r)$ by means of (19) calls for knowledge of the variation of the potential $V(r)$, since it determines the function $r_l(v)$. Expression (19) is simplified by using approximation (14). We then obtain for the ion concentration the expression^[3]

$$n_p(r) = \frac{n_0}{2} \left\{ \sqrt{1 + \frac{eV(r)}{\epsilon_0}} \pm \sqrt{1 + \frac{eV(r)}{\epsilon_0} - \frac{r_l^2}{r^2} \left[1 + \frac{eV(r_l)}{\epsilon_0} \right]} \right\}, \quad (20)$$

where the plus sign is taken if $r > r_l$ and the minus sign if $r < r_l$.

Without limitation motion, $r_l = a$ and the region $r < r_l$ would not exist.

9. Distribution of the Potential in the Vicinity of the Probe (Quasineutral Region)

The distribution of the potential in the vicinity of the probe should be obtained from the Poisson equation. At distances from the probe where $e[V(a) - V(r)] \gg kT_e$, the concentration of the electrons practically coincide with the Boltzmann concentration^[6]

$$n_e(r) = n_0 \exp \left[-\frac{eV(r)}{kT_e} \right].$$

Near the probe, where $V(r) \approx V(a)$ when $eV(a) \gg kT_e$ (large negative probe potentials), the concentration of the electrons becomes negligibly small compared with the ion concentration. Therefore we can replace n_e in the Poisson equation by the Boltzmann distribution, for all r . The ion concentration is determined by (20). We introduce dimensionless variables. Then the Poisson equation takes the form

$$\left(\frac{h}{r_l} \right)^2 \frac{1}{x^2} \frac{d}{dx} x^2 \frac{d\eta}{dx} = q(\eta, x), \quad (21)$$

$$q(\eta, x) = \frac{1}{2} \left[\sqrt{1 + \frac{\eta}{\gamma}} \pm \sqrt{1 + \frac{\eta}{\gamma} - \frac{1}{x^2} \left(1 + \frac{\eta_l}{\gamma} \right)} \right] - e^{-\eta}. \quad (22)$$

At distances exceeding several Debye radii from the probe, we can neglect the left half of (21). In other words, at such distances the plasma can be regarded as quasineutral. The quasineutrality condition is

$$\frac{1}{2} \left[\sqrt{1 + \frac{\eta}{\gamma}} \pm \sqrt{1 + \frac{\eta}{\gamma} - \frac{1}{x^2} \left(1 + \frac{\eta_l}{\gamma} \right)} \right] = e^{-\eta}. \quad (23)$$

To determine the potential of the limitation sphere η_l , we put $x = 1$ and $\eta = \eta_l$ in (23); we then get

$$\frac{\eta_l}{4e^{-2\eta_l} - 1} = \gamma. \quad (24)$$

for small γ (the electrons are "hotter" than the ions), as is the case in low-pressure cold plasmas, we obtain

$$\eta_l = 3\gamma. \quad (25)$$

Thus, in this case the potential of the limitation sphere is of the order of the energy of the ions in the unperturbed plasma. A plot of η_l against γ is shown in Fig. 6.

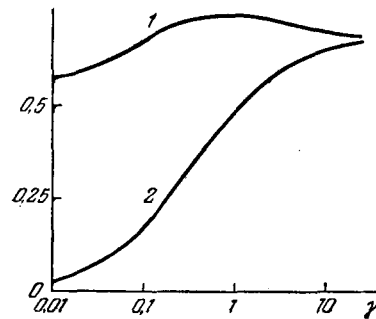


FIG. 6. $\eta_s(\gamma)$ (1) and $\eta_l(\gamma)$ (2) (spherical probe).

To find the distribution of the potential in the quasineutrality region it is convenient to solve (23) with respect to x

$$\frac{1}{x^2} = \frac{4}{1 + \frac{\eta_l}{\gamma}} \left(\sqrt{1 + \frac{\eta}{\gamma}} e^{-\eta} - e^{2\eta} \right). \quad (26)$$

The general character of the potential, obtained from this equation, can be seen from Fig. 7.* The part of the curve represented by the dashed line has no physical meaning. When $x < x_S$, (26) has no solution. This shows that in this region the quasineutrality condition is certainly not applicable. We can assume approximately $x = x_S$ on the boundary between the region of quasineutrality and the region of the space-charge

*It follows from (26) that

$$G(r) = \frac{1}{4} \frac{G(r_l)}{f - f^2},$$

where

$$f = \frac{e^{-\eta}}{\sqrt{1 + \frac{\eta}{\gamma}}}$$

is a monotonic function of the potential and consequently of the distance from the probe. It is seen therefore that $G(r)$ has one minimum for $f = 1/2$ (that is, on the limitation sphere). Thus, in the quasineutrality region the assumed form of the function $G(r)$ is justified.

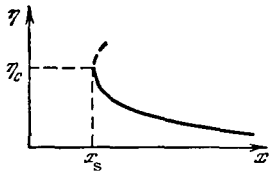


FIG. 7. Schematic variation of the potential in the quasineutrality region.

sheath^[3]. To find the limit of the layer x_s and the potential η_s on the sheath layer boundary, it is necessary to find the maximum of the right half of (26). We obtain for η_s the equation

$$\frac{1}{2\gamma} - \left(1 + \frac{\eta_s}{\gamma}\right) + 2 \sqrt{1 + \frac{\eta_s}{\gamma}} e^{-\eta_s} = 0. \quad (27)$$

The dependence of η_s and x_s on γ is shown in Figs. 6 and 8. For small γ

$$\eta_s = 0.5, \text{ and } x_s = 1.5(\gamma)^{1/4}. \quad (28)$$

The potential on the sheath for all values of γ is of the order of the electron energy in the unperturbed plasma. If the electrons are hotter than the ions, then the radius of the sheath is several times smaller than the radius of the limitation sphere.

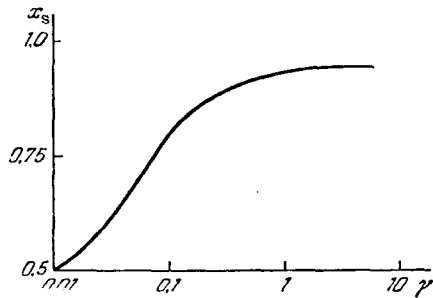


FIG. 8. Radius of sheath as a function of the parameter γ for a spherical probe.

In view of the fact that the point $x = x_s$ can be only approximately assumed to be the boundary of the sheath, and in fact the boundary of the sheath lies at $x > x_s$, it is advantageous to check the conditions under which quasineutrality is attained on the limitation sphere. The quasineutrality condition is

$$\frac{n_p - n_e}{n_p} \ll 1.$$

The concentration difference $n_p - n_e$ can be estimated by substituting in a left half of the Poisson equation (21) the solution obtained from (23). Then the condition of quasineutrality on the limitation sphere assumes the form

$$\frac{8 \left(\frac{h}{r_l}\right)^2 (\eta_l + \gamma) [1 + 2(\eta_l + \gamma) + 2(\eta_l + \gamma)^2]}{\sqrt{1 + \frac{\eta_l}{\gamma}}} \ll 1. \quad (29)$$

In the case when $\gamma \ll 1$, Eq. (29) goes over into the inequality

$$40 \left(\frac{h}{r_s}\right)^2 \gamma^{3/2} \ll 1. \quad (30)$$

For estimates we can take in place of r_s the radius

of the probe. In the most frequently encountered case of small condition (30) is usually satisfied.

10. Region of Space Charge Sheath

Inside the sheath, the potential increases rapidly on approaching the probe and the concentration of the electrons and the ions decreases, the electron concentration decreasing much more rapidly than the ion concentration. Therefore the charge density has a maximum at some distance r_p from the center of the probe. The distribution of the potential, of the concentrations n_p and n_e , and the charge density are shown schematically in Fig. 9. This type of distribution is confirmed by numerical calculation^[4]. The value of r_p can be estimated from the following considerations.

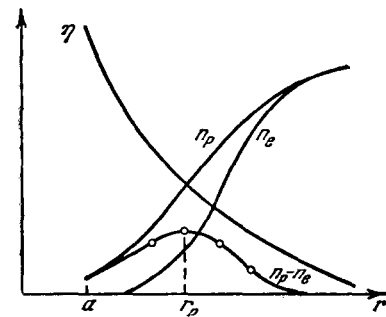


FIG. 9. Schematic distribution of the potential, of the concentration of charge particles, and the charge density in the region of the sheath.

We use the relation

$$\frac{d\eta}{dx} = \frac{\frac{dQ}{dx} - \frac{\partial Q}{\partial x}}{\partial Q / \partial \eta}. \quad (31)$$

In the region between r_s and r_p the concentration increases and $dp/dx > 0$. According to (22) $\partial p / \partial x < 0$. If the potential increases monotonically, as is confirmed by numerical calculations, then $d\eta/dx > 0$, and consequently in this region, which we shall call, following Wenzl^[4], the reflection region, we should have the inequality

$$\frac{\partial Q}{\partial \eta} = \frac{1}{4\gamma} \left[\frac{1}{\sqrt{1 + \frac{\eta}{\gamma}}} - \frac{1}{\sqrt{1 + \frac{\eta}{\gamma} - \frac{1}{x^2} \left(1 + \frac{\eta_l}{\gamma}\right)}} \right] + e^{-\eta} > 0.$$

It follows therefore that

$$1 < \left(\frac{x_s}{x_p}\right)^2 < \varphi(\gamma),$$

where

$$\varphi(\gamma) = \max \left\{ x_s^2 \frac{1 + \frac{\eta}{\gamma}}{1 + \frac{\eta_l}{\gamma}} \left[1 - \left(1 + 4\gamma \sqrt{1 + \frac{\eta}{\gamma}} e^{-\eta}\right)^{-2} \right] \right\}. \quad (32)$$

As $\gamma \rightarrow 0$ we have

$$\left(\frac{x_s}{x_p}\right)_{\max} = \sqrt{\varphi(\gamma)} = 1.38.$$

We can expect a large $d\eta/dx$ at $x = x_p$ if the probe po-

tential is sufficiently large, and the value of $(x_s/x_p)^2$ approaches its upper limit $\varphi(\gamma)$. Comparison with numerical calculations (see Sec. 11) confirms the correctness of this assumption. The value of η at which the maximum is reached in formula (32) can be regarded as the potential η_p on the inner boundary on the reflection region. As $\gamma \rightarrow 0$, $\eta_p \rightarrow 1.5$.

For $x < x_p$, there occurs an ion-layer region, in which we can neglect the concentration of the electrons compared with the concentration of the ions. In addition, we can assume in this region that the ions travel normally to the surface of the probe, that is, $\eta_l/\gamma \gg 1$. Under these conditions, the Poisson equation (21) assumes the form

$$\left(\frac{h}{r_l}\right)^2 \frac{1}{x^2} \frac{d}{dx} x^2 \frac{d\eta}{dx} = \frac{\sqrt{\gamma}}{4x^2} \frac{1 + \frac{\eta_l}{\gamma}}{\sqrt{\eta}} \quad (33)$$

The assumption that the ions move normally to the probe is well satisfied even on the outer boundary of the ion layer (for $\gamma \ll 1$). For large γ , the ions on the outer boundary of the ion layer move almost isotropically, but if the probe potential is large compared with the ion temperature, the condition for normal motion is established almost immediately beyond the boundary of the ion layer.

Equation (33) coincides with the Langmuir equation for the potential distribution in a spherical capacitor with allowance for space charge. Langmuir and Blodgett^[16] solved this equation for the case when the ions are emitted by the outer sphere, under conditions wherein the potential and the field are equal to zero on the sphere. This solution can be used if the probe potential is large compared with the potential on the layer boundary. This solution leads to the well-known "three-halves" law, which in our notation has the form

$$\left(1 + \frac{\eta_l}{\gamma}\right) \left(\frac{r_l}{h}\right)^2 = \frac{16}{9\sqrt{\gamma}} \frac{\eta_a^{3/2}}{\rho^2 \left(\frac{r_p}{a}\right)}, \quad (34)$$

where $\rho^2(r_p/a)$ are functions tabulated in [16].

11. Form of Probe Characteristic

Formula (15) can be written in the form

$$i_p = 4\pi r_p^2 e n_0 \sqrt{\frac{2kT_e}{M}} \alpha(\gamma), \quad (35)$$

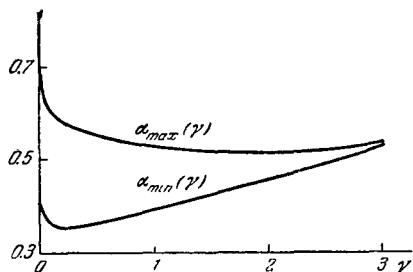


FIG. 10. $\alpha_{\max}(\gamma)$ and $\alpha_{\min}(\gamma)$ (spherical probe).

where

$$\alpha(\gamma) = \frac{\sqrt{\gamma}}{4x_c^2} \left(1 + \frac{1}{\gamma} \eta_l\right) \left(\frac{x_s}{x_p}\right)^2.$$

The maximum and minimum values of $\alpha(\gamma)$ corresponding to the maximum and minimum values of $(x_s/x_p)^2$ are shown in Fig. 10. The considerations advanced in Sec. 10 show that at sufficiently large negative probe potentials it is necessary to choose for $\alpha(\gamma)$ its maximum value. For $\gamma \rightarrow 0$, $\alpha_{\max}(\gamma) = 0.82$.^{*} To determine the current to the probe it is necessary to find the radius of the ion layer r_p . This can be done by using Eq. (34), which is best rewritten in the usual form of the "three-halves" law:

$$i_p = \frac{4\sqrt{2}}{9} \sqrt{\frac{e}{M}} \frac{V^{3/2}}{\rho^2 \left(\frac{r_p}{a}\right)}. \quad (36)$$

Formulas (35) and (36) enable us, after eliminating r_p , to determine the form of the probe characteristic:

$$\eta'^2 = \frac{9}{4} i_p^2 \rho^2(V i_p'), \quad (37)$$

where

$$\eta' = \frac{eV}{kT_e} \left(\frac{h^2}{a^2 \alpha(\gamma)}\right)^{2/3}, \quad i_p' = i_p \frac{h^2}{a^2 \alpha(\gamma)} \frac{e}{kT_e} \sqrt{\frac{2kT_e}{M}}.$$

The characteristic calculated by formula (37) is shown in Fig. 11. The same figure shows for comparison the results of numerical calculations [10,11,17]. We chose for $\alpha(\gamma)$ its maximum value. It is seen from the figure that the approximate theory agrees splendidly with the results of the numerical calculations. Some deviations begin to show up only at small probe potentials.

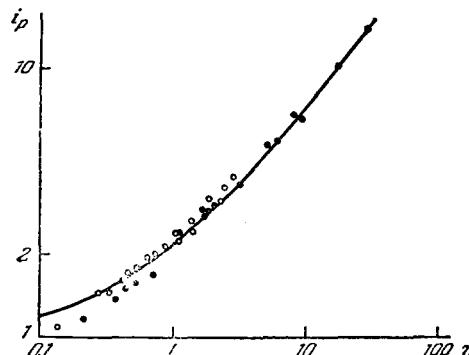


FIG. 11. Ion part of the characteristic (spherical probe). Solid curve - calculation by formula (37); points - numerical solution of the Poisson equation: $\circ - \gamma = 0.1$ ^[11], $\bullet - \gamma = 0$ ^[10,11] ($i_p = i_p'$, $\eta = \eta'$).

In the region of very small potentials (not shown in the figure), when the thickness of the sheath is small com-

[†]The value $\alpha(0) = 1$ was used in [6] as an estimate. A value $\alpha(0) = 0.43$ was obtained in [7]. This value coincides with $\alpha_{\min}(0)$ and is obtained when the reflecting layer is neglected.

pared with the radius of the probe, better agreement with the numerical calculations is obtained from formula (37) in which the minimum value is taken for α .

12. Determination of the Plasma Parameters from the Ion Part of the Characteristic

To determine the concentration of the charged particles n_0 it is necessary to determine the probe current at a sufficiently large negative probe potential V , when the electron current certainly does not come into play, so that $i = i_p$. From the given values of i_p and V we determine with the aid of (36) the value of $\rho^2(r_p/a)$, while the tables of the function $\rho^2(x)$ ^[16] yield r_p . Formula (35) is then used to determine the concentration n_0 . The ion temperature is usually unknown, so that there is some uncertainty in the value of $\alpha(\gamma)$. However, under usual discharge conditions $\gamma < 0.1$, and $\alpha_{\max}(\gamma)$, as can be seen from Fig. 10, lies between 0.8 and 0.6. To determine the electron temperature which is contained in (35), it is necessary to employ the usual method, provided it is possible to plot the part of the electronic characteristic, on which the influence of the ion current is insignificant. Otherwise it becomes necessary to use the method of differentiation, described in Sec. 4, in order to eliminate the influence of the ion current. It is possible then to employ part BC of the characteristic (see Fig. 2) near the "floating" probe potential.

Formula (36) contains the potential of the plasma relative to the probe V . If direct determination of the plasma potential (see Sec. 3) is difficult, an estimate is afforded by the fact that at the point of the ion part of the characteristic where the total probe current is equal to zero (point N on Fig. 2) we have $i_e = i_p$, that is, according to (5) and (35)

$$\frac{eV_1}{kT_e} = \ln \left[0.3 \sqrt{\frac{M}{m}} \left(\frac{a}{r_{p1}} \right)^2 \frac{1}{\alpha(\gamma)} \right], \quad (38)$$

where r_{p1} is the radius of the layer at the point N.

Assuming approximately $r_{p1} = a$, we can obtain V_1 (the potential of the plasma relative to the point N) and by the same token the potential of the plasma relative to the probe at any point of the characteristic. If $V \gg V_1$, then the inaccuracy in the determination of V_1 influences little the calculated value of the concentration. It follows from (38) that eV_1/kT_e depends little on the conditions in the plasma and depends essentially on the type of gas. This circumstance, and also the predicted value of eV_1/kT_e have been confirmed experimentally^[6]. In ^[6] there is also a comparison of the charged-particle concentrations obtained from the electron and ion parts of the characteristic for a discharge in mercury vapor.

B. CYLINDRICAL PROBE

13. Ion Current and Concentration of Charge Particles

If v_0 is the maximum impact parameter, at which an ion with initial velocity v_0 reaches the probe, then the ion current per unit length of the probe is given by the formula

$$i_p = 4\pi en_0 \int_0^\infty p_0 F_0(v_0) v_0^2 dv_0. \quad (39)$$

According to Sec. 5, $p_0^2 = G(r_l)$. We assume for simplicity that the ions away from the probe have identical energy of motion in the plane perpendicular to the probe axis, that is, we assume

$$F_0 \left(\frac{Mv_0^2}{2} \right) = \frac{M}{2\pi} \delta \left(\frac{Mv_0^2}{2} - \epsilon_0 \right). \quad (40)$$

Then we get

$$i_p = 2en_0 r_l v_0 \sqrt{1 + \frac{eV(r_l)}{\epsilon_0}}. \quad (41)$$

We proceed to determine the ion concentration. Reasoning as in Sec. 8 for the cylindrical case, and using approximation (40), we obtain

$$\left. \begin{aligned} n_p &= n_0 \left[1 - \frac{1}{\pi} \arcsin \frac{r_l}{r} \sqrt{\frac{\epsilon_0 + eV(r_l)}{\epsilon_0 + eV(r)}} \right] & \text{for } r > r_l, \\ n_p &= n_0 \frac{1}{\pi} \arcsin \frac{r_l}{r} \sqrt{\frac{\epsilon_0 + eV(r_l)}{\epsilon_0 + eV(r)}} & \text{for } r < r_l. \end{aligned} \right\} \quad (42)$$

In (42) it is necessary to take the value of the arcsine between zero and $\pi/2$ in both cases. If there is no limitation motion, then $r_L = a$ and there exist no regions $r < r_l$. In the region $r < r_l$ the Poisson equation has in dimensionless variables the form

$$\left(\frac{\hbar}{r_l} \right)^2 \frac{1}{x} \frac{d}{dx} x \frac{d\eta}{dx} = \varrho(\eta, x), \quad (43)$$

$$\varrho(\eta, x) = \frac{1}{\pi} \arcsin \frac{1}{x} \sqrt{\frac{1 + \frac{\eta l}{\gamma}}{1 + \frac{\eta}{\gamma}}} - e^{-\eta}. \quad (44)$$

For the electron concentration we assume a Boltzmann distribution, for the same reason as in the case of the spherical probe^[8].

14. Distribution of Potential in Quasineutral Region and Current in the Probe

The quasineutrality condition for the region $r < r_L$ has in dimensionless variables the form

$$\frac{1}{\pi} \arcsin \frac{1}{x} \sqrt{\frac{1 + \frac{\eta l}{\gamma}}{1 + \frac{\eta}{\gamma}}} = e^{-\eta}. \quad (45)$$

Putting $x = 1$ and $\eta = \eta_l$, we obtain the potential

for the limiting cylinder

$$\eta_l = \ln 2 = 0.69. \quad (46)$$

Let us solve Eq. (45) with respect to x :

$$\frac{1}{x} = \sqrt{\frac{1 + \frac{\eta}{\gamma}}{1 + \frac{\eta_l}{\gamma}}} \sin(\pi e^{-\eta}). \quad (47)$$

At some value of η_s , the function in the right half of (47) has a maximum. This means that when $x < x_s$ the assumption of quasineutrality is known not to be valid. To find x_s we have the equation

$$\{ \operatorname{tg}(\pi e^{-\eta_s}) - 2\pi\eta_s e^{-\eta_s} \} e^{\eta_s} = 2\pi\gamma. \quad (48)^*$$

The dependence of η_s and x_s on γ is given in Fig. 12. As $\gamma \rightarrow 0$ we have

$$\eta_s \rightarrow 0.99, \quad x_s \rightarrow 0.92. \quad (49)$$

We note that for a cylindrical probe the limitation surface lies closer to the surface of the layer than for a spherical probe. The condition of quasineutrality on the limiting cylinder can be obtained in analogy with the spherical probe (in this case we can assume $r_l \cong r_s$):

$$\left(\frac{h}{r_s}\right)^2 4(\gamma + \ln 2) [2 + \pi^2(\gamma + \ln 2)^2] \ll 1.$$

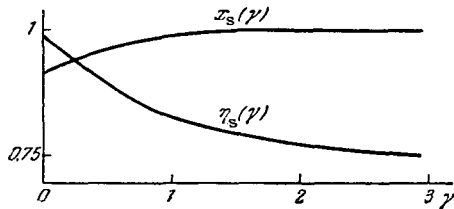


FIG. 12. $x_s(\gamma)$ and $\eta_s(\gamma)$ (cylindrical probe).

15. Region of Space-charge Sheath

Reasoning as in the case of a spherical probe (Sec. 10) we arrive at the conclusion that $\partial\rho/\partial\eta > 0$ up to the maximum of the charge density. Using formula (44), we obtain the inequality which must be satisfied by the cylinder radius corresponding to the maximum charge density:

$$1 < \left(\frac{x_s}{x_p}\right)^2 < \varphi(\gamma),$$

$$\varphi(\gamma) = \max \left\{ \frac{\gamma + \eta}{\gamma + \eta_l} \left[1 + \frac{1}{4\pi^2} \frac{e^{2\eta}}{(\gamma + \eta)^2} \right]^{-1} \right\} x_s^2. \quad (50)$$

When $\gamma = 0$

$$\left(\frac{x_s}{x_p}\right)_{\max} = \sqrt{\varphi(0)} = 1.3.$$

This value is attained when $\eta = \eta_p = 1.8$.

In the ion-layer region we can neglect for $x < x_p$

* $\operatorname{tg} = \tan$.

the concentration of the electrons and replace the arc-sine in the ion concentration by the argument, putting $\eta/\gamma \gg 1$. This is equivalent to assuming that the ions move normally to the probe inside the cylinder x_p . When $\gamma \ll 1$ such an assumption leads to an error of 15% in the concentration on the surface x_p .

Under these assumptions, the Poisson equation inside the ion layer assumes the form

$$\left(\frac{h}{r_l}\right)^2 \frac{1}{x} \frac{d}{dx} x \frac{d\eta}{dx} = \frac{1}{\pi x} \sqrt{\frac{\gamma + \eta_l}{\eta}}. \quad (51)$$

Equation (50) coincides with Langmuir's equation for a cylindrical capacitor. A solution of this equation for the case when the ions are emitted by the external cylinder was given in the paper by Langmuir and Blodgett^[16]. This solution ("three-halves" law) can be used also under the same assumptions as in the case of the spherical probe.

16. Form of Probe Characteristic and Its Processing

Formula (41) can be written in the form

$$i_p = 2\pi e r_p n_0 \sqrt{\frac{2kT_e}{M}} \alpha'(\gamma), \quad (52)$$

where

$$\alpha'(\gamma) = \frac{\sqrt{\gamma + \ln 2} x_s}{\pi x_s x_p}.$$

The maximum and minimum values of $\alpha'(\gamma)$ are given in Fig. 13. As in the case of the spherical probe, at sufficiently large negative probe potentials it is necessary to use $\alpha'_{\max}(\gamma)$.

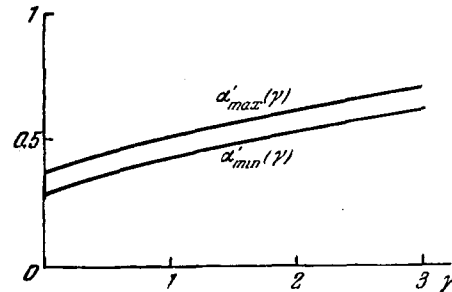


FIG. 13. $\alpha'_{\max}(\gamma)$ and $\alpha'_{\min}(\gamma)$ (cylindrical probe).

When $\gamma = 0$ we have $\alpha'_{\max}(\gamma) = 0.37$. To determine the radius of the ionic layer we use the "three-halves" law:

$$i_p = \frac{2\sqrt{2}}{9} \sqrt{\frac{e}{M}} \frac{V^{3/2}}{\alpha\beta^2 \left(\frac{r_p}{a}\right)}. \quad (53)$$

After eliminating r_p from (52) and (53), we obtain the form of the probe characteristic

$$\eta^{3/2} = \frac{9}{2} i_p \beta^2 (2i_p), \quad (54)$$

where

$$\eta' = \frac{eV}{kT_e} \left[\frac{h^2}{a^2 \alpha'(\gamma)} \right]^{2/3}, \quad i_p' = \frac{i_p h}{\frac{kT_e}{e} \sqrt{\frac{2kT_e}{e} \frac{a}{h} \alpha'(\gamma)}}$$

The characteristic calculated by formula (54) is shown in Fig. 14. The characteristic is processed in the same way as in the case of a spherical probe (see Sec. 12). The roles of formulas (35) and (36) are now assumed by (52) and (53). When $\gamma < 0.1$ we have $\alpha'_{\max}(\gamma) \approx 0.4$. Tables of the functions $\beta^2(r_p/a)$ are contained in [16,18]. The plasma potential relative to the isolated probe is obtained from the same considerations as for the spherical probe:

$$\frac{eV_1}{kT_e} = \ln \left[0.3 \sqrt{\frac{M}{m} \frac{a}{r_{p1}} \frac{1}{\alpha'(\gamma)}} \right]. \quad (55)$$

In [8,19] there is a detailed comparison of the concentrations of the charged particles, the electron temperatures, and the space potentials obtained by processing the electronic and ionic parts of the characteristic for discharges in mercury vapor [8] and in argon [19]. The agreement should be regarded as good.*

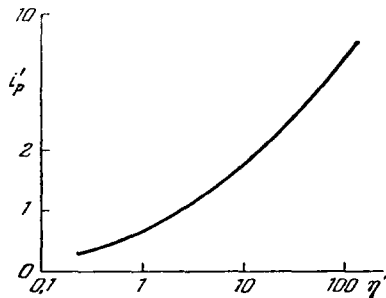


FIG. 14. Ion part of the characteristic. Cylindrical probe. Calculation by formula (54).

III. THE METHOD OF TWO PROBES

17. Principles of the Method

In those cases when there is no electrode with specified potential in the discharge gap (decaying plasma, high-frequency discharge) direct use of the single-probe method is impossible. One way of overcoming this difficulty is to use the method of two probes [20-23], which consists in the following: two identical probes are introduced into the discharge gap and the current in the probe circuit is measured as a function of the potential difference between the probes. The approximate form of the resultant probe characteristic is

*We note, however, that too high a coefficient of (52) was used in [8], thus reducing the concentration in the ion part by a factor of 2.5, so that the space potential for the electron part was determined from the deviation from linearity, and not from the crossing of the asymptotes, and the electron concentration was underestimated. In [19] the concentration in the ion part was calculated by using (52) with the correct coefficient, but no account was taken of the space-charge thickness.

shown in Fig. 15. If the probes are identical and the plasma homogeneous, then the characteristic is symmetrical with respect to the point where the current vanishes. Δ is equal in magnitude to the potential difference between the portions of the plasma in which the probes are located. Obviously, the currents flowing in the probes should be identical in magnitude and opposite in sign. Therefore the potential of the more positive probe can be only slightly higher than the potential of the floating probe, owing to the steep increase of the electron current with increasing probe potential. When the difference in potential between the probes is large (regions AB and CD of Fig. 15), practically the entire potential difference is equal to the potential of the more negative probe (relative to the floating probe). Then practically the entire current in the negative probe is due to ions. Thus, if we align those points of the two-probe and single-probe characteristics in which the current in the circuit is equal to zero (points N of Figs. 2 and 15), then these characteristics coincide in the far ion parts (AB).

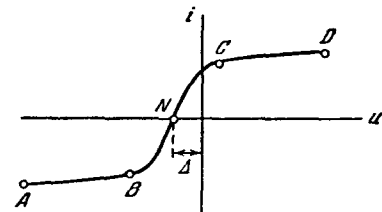


FIG. 15. Schematic form of two-probe characteristic.

The form of the characteristics in the region BC can be obtained by using the fact that the probe currents are equal in magnitude:

$$i(u) = i_p(V') - i_0 e^{-\frac{eV'}{kT_e}} = i_0 e^{-\frac{eV''}{kT_e}} - i_p(V''), \quad (56)$$

$$u - \Delta = V' - V'', \quad (57)$$

where v' and v'' are the potentials of the plasma relative to the first and second probes, and $i(u)$ is the current in the two-probe circuit. For the electron we use formula (5). If we eliminate V' and V'' from (56) and (57), we obtain the equation of the characteristic $i(u)$. For this purpose it is necessary to know the dependence of the ion current on the probe potential. If we assume the ion current to be independent of the potential, then we obtain for the characteristic an equation in the form [20]

$$i(u) = i_p \operatorname{th} \frac{e(u - \Delta)}{2kT_e}. \quad (58)*$$

This expression agrees with the form of the characteristic in the region BC. At large u it leads to saturation, this being the consequence of failure to take

*th = tanh.

into account the dependence of the ion current on the potential.*

18. Determination of the Plasma Parameters from the Two-probe Characteristic

Several methods were proposed to determine the electron temperature T_e [21,20]. The simplest method uses the slope of the two-probe characteristic at the point where $u = \Delta$. We shall assume that the probes and the plasma sections adjacent to them are identical. Differentiating (56) with respect to u and putting $u = \Delta$, and consequently $V' = V'' = V_1$, making use of the fact that at the point $u = \Delta$ we have as a result of (57) and the equivalence of the probes the condition

$$\frac{dV'}{du} = -\frac{dV''}{du} = \frac{1}{2},$$

and recognizing that when $u = \Delta$ the electron current is equal to the ion current, we get

$$T_e = \frac{e}{k} \frac{i_p(V_1)}{2 \left(\frac{di}{du} \right)_N - \left(\frac{di_p}{dV} \right)_N}. \quad (59)$$

From (59) we can determine the electron temperature by measuring the slope of the characteristic at $u = \Delta$. The ion current and its derivative at the potential of the isolated probe can be determined by extrapolation from the large potentials, at which the ion current coincides with the total current in the two-probe circuit, and

$$\frac{di_p}{dV} \approx \frac{di_p}{du}.$$

The extrapolation method should be based on the form of the dependence of the probe ion current on the probe potential relative to the plasma. As follows from Secs. 11 and 16, this dependence is complicated and has a different form for different discharge parameters. Therefore it is convenient to use (59) in practice in those cases when the slope of the remote parts of the two-probe characteristic is small compared with the slope at the point where the current is equal to zero. In this case the quantity $(di_p/dV)_{V_1}$ can be neglected, and the $i_p(V_1)$ depends little on the method of extrapolation, and can be obtained for example by linear extrapolation.†

In the case when the characteristic is not symmetrical, which may be the consequence of the inequality

*The form of the characteristic was obtained in [24] under the assumption that the ion current in the probe depends linearly on the probe potential.

†More complicated extrapolation methods were proposed in many papers [20,24]. These postulated in fact a linear dependence of the probe ion current on the probe potential relative to the plasma. Starting from this dependence, the authors found the form of the two-probe characteristic and the corresponding extrapolation method. The quantity $(di_p/dV)_{V_1}$ was determined in this case from the slope of the remote part of the two-probe characteristic.

of the probes or of the charged-particle concentrations around the probes, (59) cannot be used. In this case (56) is replaced by

$$i(u) = i_0'' e^{\frac{eV''}{kT_e}} - i_p''(V'') = i_p'(V') - i_0' e^{\frac{eV'}{kT_e}}. \quad (60)$$

We obtain from this a formula in place of (59) for the case of an asymmetrical characteristic [25]:

$$\frac{di}{du} = \left\{ \left(\frac{di_p''}{dV''} + \frac{e}{kT_e} i_p'' \right)^{-1} + \left(\frac{di_p'}{dV'} + \frac{e}{kT_e} i_p' \right)^{-1} \right\}^{-1}. \quad (61)$$

All the quantities in the right half of (61) are taken for the values of the potential at which the current in the two-probe circuit is equal to zero. As in the case of identical probe, it is convenient to use (61) in practice when the slopes of the remote parts of the characteristics are small compared with the slope at the point N. In this case (61) assumes the form

$$T_e = \frac{e}{k} \frac{i_p' i_p''}{i_p' + i_p''} \left(\frac{di}{du} \right)_N^{-1}. \quad (62)$$

Another method of finding the electron temperature consists in the following [20].

Using (57) and (60) we get

$$\ln \left(\frac{i_p' + i_p''}{i_e} - 1 \right) = A + \frac{e}{kT_e} u, \quad (63)$$

where

$$A = \ln \frac{i_0''}{i_0'} e^{-\frac{e\Delta}{kT_e}}.$$

i_p' , i_p'' , and i_e are obtained from the two-probe characteristic, as shown in Fig. 16 (we note that in this method the ion current must be extrapolated). If we plot the left half of (63) as a function of u , we obtain the electron temperature from the slope of the resultant line, and knowing T_e we can determine the concentration of the electrons by using the already mentioned equality of the ion parts of the two-probe and single-probe characteristics, provided the two are aligned at the point N. The method described in Secs. 11 and 16 can be used.

The method proposed in [20-22] for determining the concentrations is incorrect, since it is based on the Langmuir theory for the ion current. Frequently comparisons of the two-probe method with the single-probe method [23,26,27] (in the case when the latter is applicable) and with microwave methods [28,29] have shown good agreement between the results.

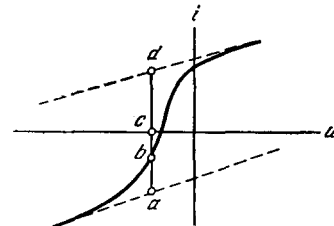


FIG. 16. Illustrating the determination of the electron temperature by the method of Malter and Johnson: $ab = i_e'$, $ac = i_p''$, $cd = i_p''$.

19. The Counterprobe and Triple-probe Methods

In this section we consider methods of obtaining the single-probe characteristic using a two-probe circuit. The idea of the counterprobe method consists in the following^[30]. If the dimensions of one probe greatly exceed those of the other, then considerable changes in the potential of the smaller probe are possible. Its potential may become higher than that of the isolated probe and even higher than the plasma potential, whereas the potential of the larger probe remains practically unchanged at approximately the potential of the isolated probe. This can be understood from the following considerations: since one of the probes is small, the current in the two-probe circuit should be small. Therefore the potential of the larger probe cannot differ greatly from the potential of the isolated probe. In the case of sufficiently large difference in dimensions, even the electron current in the small probe, which is at the plasma potential, can become offset by the current in the large probe, the potential of which is somewhat lower than the floating probe potential. The probe characteristic then turns into the single-probe characteristic of the small probe and can be processed by the usual Langmuir method. To find a criterion by which to judge whether the larger probe is sufficiently large to serve as a counterprobe, we use Eq. (60), assuming the first probe to be large and the second small.

Let us differentiate both halves, neglecting the variation of the ion current compared with the variation of the corresponding electron current. We then obtain

$$\left| \frac{dV'}{dV''} \right| = \frac{i_0'}{i_p(V_1)} \quad (64)$$

Equation (64) has been written out for the case where the potential of the small probe is close to the space potential, and the counterprobe is at the potential of the floating probe V_1 . The characteristic will be practically that of a single probe if $dV' \ll dV''$. If the probe and the counter probe are under identical conditions, then using (11), (64), and the fact that

$$i_0 = \frac{1}{4} en_0 \bar{v}_e S,$$

we obtain the criterion for the applicability of the counterprobe method in the form

$$\frac{S'}{S''} \gg \sqrt{\frac{M}{m}}, \quad (65)$$

where S' and S'' are the surface areas of the counterprobe and the probe. If the counterprobe is in a region with reduced charged-particle concentration, then condition (65) is insufficient. The need for introducing the counterprobe directly in the discharge gap, where it unavoidably distorts the plasma, is the main shortcoming of this method.

In^[24,31] there is proposed a triple-probe method, which, like the counterprobe method, makes it possible to obtain the single-probe characteristic. Three probes

are connected as shown in Fig. 17. In each measurement, the potentiometer slide wire is set in a position such that the current in the circuit of probe 3 is equal to zero. This means that probe 3 is always at the floating-probe potential. The dependence of the current in the circuit of probes 1 and 2 on the potential V_2 is the single-probe characteristic of probe 2, which, in principle, can be processed by the methods described in Chapters I and II. However, if probes 1 and 2 are comparable in dimensions, then only the very start of the electron part of the characteristic is obtained. In order to obtain the entire electron part of the single-probe characteristic of probe 2, probe 1 must be so much larger than probe 2 that the ion current in probe 1 balances out the electron current in probe 2 at the space potential. This calls for a fixed ratio of the areas:

$$\frac{S'}{S''} \gg \sqrt{\frac{M}{m}}. \quad (66)$$

(The criterion given in^[31] is incorrect, because the authors used the Langmuir theory for the ion current.)

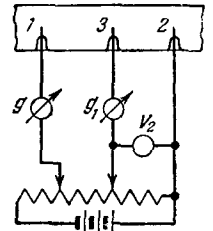


FIG. 17. Diagram of the triple-probe method.

Criterion (66) is less stringent than the criterion for the applicability of the counterprobe method (65). The reason for it is that in the three-probe method there is no need to maintain the potential of probe 1 constant. The fact that the entire electron part of the single-probe characteristic is obtained in the three-probe method makes it possible to obtain the energy distribution of the electrons with the aid of formula (4).

A modification of the triple-probe method was used in^[32], where the potential difference between probes 1 and 2 was kept constant, and the area of the smaller probe 2, which was at a higher potential relative to the plasma than the larger probe 1, was varied. The dependence of the current in the two-probe circuit and of the potential V_2 on the area of probe 2 makes it possible to determine the electron concentration and temperature. An inconvenience of this method is the use of a probe of variable length. In addition, at small probe dimensions, distortions may be produced as a result of the influence of the insulation.

20. Influence of High-frequency Field on the Probe Characteristic

Measurement of field intensity. One of the main uses of the two-probe method is for a high-frequency discharge. A typical two-probe measurement circuit

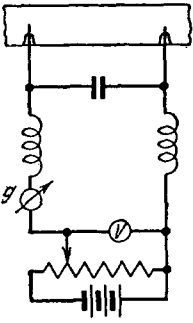


FIG. 18. The two-probe method used in a high-frequency discharge.

is shown in Fig. 18. The choke and the capacitor keep the high-frequency current component out of the measuring circuit. The high-frequency component may be the result of periodic variations of the potential difference between the sections of the plasma adjacent to the probes. Owing to the nonlinearity of the probe characteristic, this variable potential difference distorts also the dc component of the current in the probe circuit.

The distortion can be reduced by locating the probes in an equipotential plane. Such an arrangement is not convenient in narrow tubes, since the plasma properties vary in the radial direction. Too small a distance between probes can lead to their mutual screening. It is therefore advantageous sometimes to locate the probes along the axis of the discharge. Let us consider the influence of the high frequency field on the form of the probe characteristics^[33]. Since the ion current depends little on the probe potential, the high frequency field hardly exerts any influence on it. Therefore the method described above for determining the concentration using the ion part of the characteristic can be used also in a high frequency discharge. The electron current depends strongly on the potential, and therefore the high frequency field can influence the form of the characteristic near the plane where the probe current is equal to zero. If the frequency is not too large, then the current in the probe at each instant of time is determined by Eq. (58). (We assume for simplicity that the ion current does not depend on the potential and that the probes, as well as the concentration and temperature of the plasma electrons near the probes, are identical.) By Δ we must mean the instantaneous difference of potentials between the portions of the plasma adjacent to the probes:

$$\Delta = E_d d \sin \omega t + \Delta_0,$$

where E_d is the maximum value of the projection of the intensity of the high-frequency field on the line joining the probes, Δ_0 is the DC component of the potential difference, and d is the distance between probes.* To obtain the experimentally measured dc

*Such an adiabatic analysis is applicable if the time necessary for the electron to pass through the perturbed region is much shorter than the period of the oscillations. At a temperature $T_e \sim 10^4$ °K and a probe radius 0.1 mm, this holds up to a frequency $\nu \sim 10^9$ cps.

component of the two-probe current we average (58) over the time. We then get

$$i(u) = i_p \int_0^1 \text{th} \frac{e(u - \Delta_0 - E_d d \sin 2\pi x)}{2kT_e} dx. \quad (67)$$

It is seen from (67) that the current is equal to zero at the point where $u = \Delta_0$, that is, the high frequency field does not cause a shift of the characteristic. However, the slope of the characteristic at the point where the current is equal to zero depends on the high frequency field. Namely,

$$\left(\frac{di}{du}\right)_{u=\Delta} = \frac{e}{2kT_e} i_p \int_0^1 \frac{dx}{\text{ch}^2 A \sin \pi x}, \quad (68)^*$$

where $A = eE_d d / 2kT_e$. From (68) we see that the high frequency field is insignificant only if $A \ll 1$. The numerical values of the integral are 1, 0.89, 0.67, 0.36 for $A = 0, 0.5, 1, \text{ and } 2$, respectively. In^[33,34] it was proposed to use formula (68) for the measurement of the intensity of the high frequency field in the discharge. To this end, two probes on a ground-glass joint are located first in an equipotential plane ($E_d = 0$) and the electron temperature T_b is measured. The probes are then rotated about the axis, and the value of E and the field intensity E_d are determined with the aid of (68).

A different method of measuring the field intensity was proposed in^[35]. The triple-probe circuit employed consists in paralleling the identical probes 1 and 2 and making their total area equal to the area of probe 3, which is placed between them. A two-probe characteristic is plotted for probe 3 and probes 1–2. The presence of a high-frequency field causes the probe characteristic to shift and the field is determined from this shift. However, the expression obtained for the shift is incorrect, since it was erroneously assumed that the potential difference between the double probe 1–2 and the plasma at the probe 3 is independent of the time. A correct expression for the current in the probe circuit averaged over the period (under the usual assumption that $i_p = \text{const}$) is:

$$\overline{i(u)} = i_p \int_0^1 \frac{1 - e^{-\frac{eu}{kT_e}} \text{ch} \left(\frac{eE_d d}{kT_e} \sin 2\pi x + \frac{e\Delta_0}{kT_e} \right)}{1 + e^{-\frac{eu}{kT_e}} \text{ch} \left(\frac{eE_d d}{kT_e} \sin 2\pi x + \frac{e\Delta_0}{kT_e} \right)} dx, \quad (69)$$

where u is the potential difference between the double probe 1–2 and probe 3, Δ_0 is the dc component of the difference in the plasma potentials near probes 1 and 2, and d is the distance between probes 1 and 3 or 2 and 3.

Formula (69) shows that the presence of a high frequency field (as well as the presence of a dc component Δ_0) causes a shift in the characteristic ($u \neq 0$ with $\dot{i} = 0$). This method has so far not been used with the correct formula (69).

In^[28] attention was called to one feature of probe

*ch = cosh.

measurement in a high-frequency discharge, namely that the plasma of the high-frequency discharge can have a large alternating potential relative to ground. The capacitance of the probe leads relative to ground can be sufficiently large (particularly if account is taken of the fact that the probe leads are usually shielded). The ac voltage applied between the plasma and the ground is rectified because of the nonlinearity of the current-voltage characteristic of the probe. This leads to the appearance of additional direct current in the measuring probe circuit, and to an overestimate of the concentration of the charge particles measured by the two-probe method. The role of this effect has been insufficiently studied, but the data given in [28] show that the distortion is not too large.

IV. USE OF THE PROBE METHOD UNDER MORE COMPLICATED CONDITIONS

21. Probe Measurements in Mixtures

If the plasma contains two kinds of positive ions, with different masses, then the theory of the ion part of the characteristic must be modified. If the charges and ion energies are identical, then the Poisson equation (21) [and (43)] are written in the same form also in the case of a mixture, and the electron concentration is $n_0 = n_{p1} + n_{p2}$, where n_{p1} and n_{p2} are the ion concentrations of the components. Thus, the distribution of the potential around the probe will be the same as in the case when only one kind of ion is present. Let us consider by way of an example the case of a cylindrical probe [36].

According to Sec. 16 we have the following expression for the ion current per unit probe length:

$$i_p = i_{p1} + i_{p2} = 2\pi er_p \sqrt{2kT_e} \alpha'(\gamma) \left(\frac{n_{p1}}{\sqrt{M_1}} + \frac{n_{p2}}{\sqrt{M_2}} \right). \quad (70)$$

To determine the radius r_p of the ion layer, we use the "three halves" law, which in the presence of two kinds of ions takes the form

$$i_{p1} \sqrt{M_1} + i_{p2} \sqrt{M_2} = \frac{2\sqrt{2}}{9} V e^{-\frac{V^{3/2}}{a\beta^2 \left(\frac{r_p}{a}\right)}}. \quad (71)$$

From this we obtain for the radius of the ion layer r_p the relation

$$\frac{r_p}{a} \beta^2 \left(\frac{r_p}{a}\right) = \frac{1}{9\pi} \frac{1}{\sqrt{kT_e}} \frac{1}{e n_0} \frac{1}{a^2 \alpha'(\gamma)} V^{3/2}. \quad (72)$$

By measuring the total ion current i_p at a large negative potential V , and by determining the electron concentration n_0 and T_e from the electron part of the characteristic, we can find n_{p1} and n_{p2} from (70) and from the condition that the plasma be neutral.

It must be borne in mind that even small errors in the determination of n_0 from the electron part of the characteristic can in some cases lead to large errors in determination of the concentrations of the components. This method, however, can be used to obtain qualitative results [37,38].

22. Probe Measurements in Electronegative Gases

This question has been treated in only a few investigations, and the experimental material is very scanty [3,39-44]. We consider first the part of the characteristic adjacent to the space potential and corresponding to small negative probe potentials. If

$$\delta \equiv \frac{n_-}{n_e} \ll \sqrt{\frac{M_- T_e}{m T_-}}$$

(the subscript "-" pertains to negative ions), then the negative-ion current is much smaller than the electron current in this part of the characteristic. If we recognize that usually $T_- \sim T_p \ll T_e$ then, say for oxygen, the influence of the negative ions will not be felt even a at the space potential if $n_-/n_e \ll 10^3$. At negative probe potentials, the negative-ion current will make an even smaller relative contribution. In this case we can obtain n_e and T_e from this part of the characteristic by the usual method. However, even if the above-mentioned criterion is satisfied but $\delta \gg 1$, then the presence of a large number of negative ions will be manifest in the fact that the ratio of the electron saturation current to the saturation current of the positive ions will greatly decrease [from the condition of quasineutrality of the plasma $n_p = n_e + n_- = n_e(1 + \delta)$]. Therefore, to process the electronic part of the characteristic by the Langmuir method it may be necessary to eliminate the positive-ion current (Sec. 4). In fact, when working with electronegative gases there are frequently striations in the plasma and the electron distribution deviates appreciably from Maxwellian. In these cases it is advantageous to seek the electron energy distribution function by using formula (4a). An example of a distribution obtained in this manner for a discharge in oxygen [40] is shown in Fig. 19. The narrow peak at low energies corresponds to the negative ions. In the presence of electrons and negative singly-charged ions, formula (4a) is transformed into

$$\begin{aligned} V \bar{V} \frac{d^2}{dV^2} (-j_e) \\ = \frac{e^2}{2\sqrt{2}} \left[\sqrt{\frac{e}{m}} n_e f'_0(eV) + \sqrt{\frac{e}{M_-}} n_- f'_{0-}(eV) \right]. \end{aligned}$$

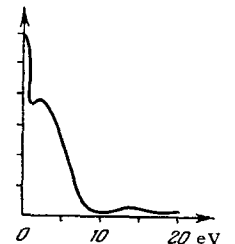


FIG. 19. Energy distribution of negatively charged particles in a discharge in oxygen in the presence of striations [40].

The concentration ratio obtained for the case corresponding to Fig. 19 by separating the particle re- sponding to the negative ions and integrating over the energies, with allowance for the mass difference, was $n_-/n_e \sim 20$.

The theory of the ion part of the characteristic in the presence of negative ions was presented for a spherical probe in [39]. We use here the method developed in Ch. II. For simplicity we assume that

$$\frac{T_-}{T_e} = \frac{T_p}{T_e} = \gamma.$$

For a spherical probe this method leads to the following results for $\delta \gg 1$:

$$\eta_s = 0.75\gamma, \quad x_s = 0.96, \quad 1 < \left(\frac{x_s}{x_p}\right)^2 < 1.35.$$

As can be seen, the boundary of the layer is in this case very close to the limitation sphere. For the current in the probe we obtain

$$i_p = \frac{4\pi r_p^2 e n_{p0} v_p}{4} \kappa(\delta, \gamma). \quad (73)$$

When $\delta \gg 1$ we get $1.6 < \kappa < 2.2$.

The result of [39], obtained from qualitative considerations, differs from (73) by a numerical factor.

In analogous fashion we obtain for a cylindrical probe with $\delta \gg 1$

$$i_p = \frac{2\pi r_p e n_{p0} v_p}{4} \kappa', \quad 1.3 < \kappa' < 1.6. \quad (74)$$

The results obtained show that when there are much fewer electrons than negative ions, the potential on the boundary of the layer is of the order of kT_p/e and the velocity of the positive ions on the boundary of the layer is of the order of the thermal velocity.

The radius of the ion layer r_p is determined from the "three halves" law.*

The plasma potential relative to the isolated probe V_1 is determined for $\delta \gg 1$ from the equation

$$\left(\frac{r_p}{a}\right)^2 \kappa = \sqrt{\frac{T_e M}{m T_p}} \frac{1}{\delta} e^{-\frac{eV_1}{kT_e}} + e^{-\frac{eV_1}{kT_p}}. \quad (75)$$

With increasing concentration of the negative ions, V_1 decreases and becomes of the order of kT_p/e when $\delta \gg \sqrt{T_e M / m T_p}$.

We note that the theory developed above does not make it possible to determine all the plasma parameters of interest to us. However, if T_- and T_p can be estimated from some supplementary considerations, then in the case when

$$1 \ll \delta \ll \sqrt{\frac{M - T_e}{m T_-}},$$

it is possible to determine n_e and T_e from the electron part and n_p from the ion part.

*The use of the "three halves" law for $r < r_p$ is valid if positive ions predominate in this region. When the potentials reached are approximately equal to kT_e/e , the electron concentration changes insignificantly, whereas the ion concentration decreases by a factor $(T_e/T_p)^{1/2}$. Therefore the condition $\delta \gg 1$ is still insufficient to permit neglect of the electron concentration in the region $r < r_p$. To this end it is necessary to satisfy the more stringent condition $\delta \gg (T_e/T_p)^{1/2}$.

23. Probe Measurements in the Presence of Magnetic Fields

The theory of probe measurements in the presence of a magnetic field has been treated in several works [3,45,46], but no reliable theory of probe measurements in a magnetic field exists so far. In [45] there is calculated the electron current in an infinite cylindrical or plane probe under the assumption that at some distance d from the probe the charged particles have the same concentration in velocity distribution as in the unperturbed plasma. In a layer of thickness d , the particles move without collision under the influence of the electric and magnetic fields. If the surface of the probe is parallel to the magnetic field, then only those particles whose Larmor radius is larger than d will strike the probe. With increasing magnetic field, the number of such particles decreases and the current in the probe also decreases. At negative probe potentials, the influence of the magnetic field on the electron current decreases with increasing absolute value of the potential. The reason for it is that at large negative potentials the probe receives only the fast electrons, whose Larmor radius is large. The value of d itself remains undetermined, and it is proposed to assume that it is of the order of the mean free path λ . No account is taken here of several factors: the particles whose Larmor radius is smaller than λ can reach the probe as a result of diffusion; an important role may be played in the magnetic field by particle currents moving along the magnetic force lines, and consequently the finite size of the probe is essential; the depletion of the plasma at a distance d may also become essential.

In the case when the surface of the plane probe is perpendicular to the direction of the magnetic field, the magnetic field at first glance does not affect the probe current at all. This circumstance could yield a good method of measuring the plasma parameters in a magnetic field. However, with the increasing magnetic field, the depletion of the plasma in the cylindrical region terminated by the probe may become significant. The reason for it is that the particles rapidly leave this region and go to the probe, while the diffusion from the neighboring regions is made difficult by the magnetic field.

An approximate expression is derived in [3] for the electron current when the probe is at a probe potential somewhat higher than the plasma potential. In this derivation explicit account is taken of the diffusion character of the motion of the electrons transversely to the magnetic field, of the depletion of the plasma in the vicinity of the probe, and of the finite size of the probe. To obtain the solution, it is necessary to use the diffusion equation also for the direction along the magnetic field. The problem is formulated in this fashion. The motion is assumed to be due to diffusion up to a distance on the order of the mean free path λ

from the probe, in the direction of the magnetic field, and up to a distance equal to the Larmor radius R from the probe in a perpendicular direction. If the probe potential is sufficiently positive to prevent the ions from reaching the probe, then the ions in the vicinity of the probe can be assumed to have a Boltzmann distribution. If, in addition, we assume the plasma to be quasineutral, then

$$n \equiv n_p = n_e = n_0 e^{\frac{eV}{kT_p}}, \quad (76)$$

where V , as usual, is the potential of the unperturbed plasma relative to the given point, so that in the case under consideration $V < 0$. In the diffusion region, the electron currents to the probe in the longitudinal and transverse directions are given by the formulas

$$\left. \begin{aligned} j_{\parallel} &= -D_{\parallel} \left(\frac{\partial n}{\partial z} - \frac{e}{kT_e} n \frac{\partial V}{\partial z} \right) = -D_{\parallel} (1 + \gamma) \frac{\partial n}{\partial z}, \\ j_{\perp} &= -D_{\perp} \left(\nabla_{\perp} n - \frac{e}{kT_e} n \nabla_{\perp} V \right) = -D_{\perp} (1 + \gamma) \nabla_{\perp} n, \end{aligned} \right\} \quad (77)$$

where $\gamma = T_p/T_e$, and the z axis coincides with the direction of the magnetic field.

Neglecting the ionization in the perturbed region, we can write $\text{div } \mathbf{j} = 0$, or

$$\frac{\partial^2 n}{\partial z^2} + \alpha \left(\frac{\partial^2 n}{\partial x^2} + \frac{\partial^2 n}{\partial y^2} \right) = 0, \quad \alpha = \frac{D_{\perp}}{D_{\parallel}}. \quad (78)$$

Equation (78) can be reduced to the Laplace equation by introducing the variable $s = \sqrt{\alpha z}$. Let us surround the probe with an infinitely long cylindrical surface, the axis of which is directed along the magnetic field. The current in the probe is given by the formula

$$i_e = e \int \mathbf{j}_{\perp} d\sigma = e (1 + \gamma) \sqrt{\alpha} D_{\parallel} \int \nabla_{\perp} n d\sigma_s. \quad (79)$$

Here $d\sigma_s$ is the cylinder area element in coordinates s , x , and y . For the side surface of the cylinder we have $d\sigma_s = \sqrt{\alpha} d\sigma$. To calculate the integral (79) we can use the following electrostatic analogy. If the body has a potential V then, according to the Gauss theorem, the charge on the body is, on the one hand,

$$-\frac{1}{4\pi} \int \nabla V \cdot d\sigma,$$

and on the other hand it is equal to CV , where C is the capacitance of the body. Thus,

$$\int \nabla V \cdot d\sigma = 4\pi C (V_0 - V),$$

where V_0 is the potential at infinity.

In our case the analog of the potential is the concentration n , which, like the potential itself, satisfies the Laplace equation. Therefore

$$\int \nabla_{\perp} n d\sigma_s = 4\pi C (n_0 - n_1),$$

where n_1 is the concentration on the boundary of the diffusion region. Thus,

$$i_e = e (1 + \gamma) \sqrt{\alpha} D_{\parallel} 4\pi C (n_0 - n_1). \quad (80)$$

The motion of the particles from the boundary of the diffusion region to the probe is almost free (it is assumed that $\gamma \ll 1$, and the weak positive potential which drives the ions away does not influence the motion of the electrons). Consequently

$$i_e = \frac{n_1 \bar{v}_e S}{4}, \quad (81)$$

where S is the area of the probe. Eliminating n_1 from (80) and (81), we get

$$i_e = \frac{en_0 \bar{v}_e S}{4} \left(1 + \frac{\bar{v}_e S}{16 \sqrt{\alpha} D_{\parallel} \pi C} \right)^{-1}. \quad (82)$$

In the limiting case of strong magnetic fields $\sqrt{\alpha} \ll S/16\lambda C$ (where λ is the mean free path along the field), formula (82) assumes the form

$$i_e = 4\pi en_0 \sqrt{\alpha} D_{\parallel} C. \quad (83)$$

It is seen from (83) that the currents in probes of equal shape or dimensions differ only as a result of the difference in the capacitances C . It must be emphasized that in Eqs. (80)–(83) C stands for the capacitance of the body whose surface is obtained by multiplying all the longitudinal dimensions of the diffusion region by $\sqrt{\alpha}$. Therefore the value of C of the same probe depends on the probe orientation relative to the magnetic field. For a disc of radius a oriented perpendicular to the field, the boundary of the diffusion region can be approximated by the surface of an ellipsoid of revolution of radius $a + R$ (where R is the Larmor radius) and height λ . To calculate the capacitance C , the longitudinal dimensions should be multiplied by $\sqrt{\alpha}$. If the field is so large that $\lambda\sqrt{\alpha} \ll a$ and $R \ll a$, then C is the capacitance of a disc of radius a , that is, $C_{\perp} = 2a/\pi$. Substituting this value in (83), we find that the presence of a magnetic field decreases the electron current to a plane probe oriented perpendicular to the field in a ratio R/a (if we choose for $\sqrt{\alpha}$ its classical value R/λ). This is connected with the aforementioned depletion of the plasma ahead of the probe.

We now consider a disc of radius a , oriented parallel to the magnetic field. C is in this case the capacitance of an ellipsoid with major semiaxis a and minor semiaxes R and $(a + \lambda)\sqrt{\alpha}$. For the case $\lambda\sqrt{\alpha}/a \ll 1$ and $\sqrt{\alpha} \ll 1$, its capacitance is equal to

$$C_{\parallel} = a \left[\ln \frac{\beta}{\left(1 + \frac{\lambda}{a}\right) \sqrt{\alpha}} \right]^{-1},$$

where $\beta = 4$ if $\lambda/a \ll 1$ and $\beta = 2$ if $\lambda/a \gg 1$. For the ratio of the electron currents in parallel and perpendicular probes we obtain

$$\frac{(i_e)_{\perp}}{(i_e)_{\parallel}} = \frac{C_{\perp}}{C_{\parallel}} = \frac{2}{\pi} \ln \frac{\beta}{\left(1 + \frac{\lambda}{a}\right) \sqrt{\alpha}}. \quad (84)$$

It is seen from (84) that the ratio of the currents de-

pends little on the magnetic field. The ratio of the electron current at space potential to the ion current at large negative probe potentials will be

$$\frac{(i_e)_\perp}{i_p} \cong \sqrt{\frac{M}{m}} \frac{\lambda}{a} \sqrt{\alpha}. \quad (85)$$

It is assumed here that the radius of the probe is larger than the Larmor radius of the electrons and smaller than the Larmor radius for ions. For the ion current we have used formula (11).

All the formulas presented contain α — the ratio of the diffusion coefficients transverse to and along the magnetic field. The classical expression for α in strong fields is

$$\alpha = \frac{R^2}{\lambda^2}. \quad (86)$$

However, in strong magnetic fields, there can be anomalous diffusion connected with the different instabilities in the plasma^[3,47]. This raises additional difficulties when using probes in a strong magnetic field. Even if the coefficient of transverse diffusion is known, Eq. (83) still does not make it possible to determine the concentration of electrons n_0 , for in a magnetic field the point of inflection on a semilog characteristic can be weakly pronounced, and the space potential may therefore be unknown. In addition, there is no method for determining the electron temperature. At the present time probes can be used only in not too strong magnetic fields, namely when the Larmor radius for the ions is much larger than the probe dimensions^[48]. In this case the magnetic field does not influence the ion part of the characteristic and it is possible to employ the theory presented in Ch. II. The usual method of determining the electron temperature T_e can be used only if the Larmor radius of the electrons that constitute the current flow at the given point of the characteristic is large compared with the probe dimensions. Since the current is produced by faster and faster electrons with increasing negative probe potential, it is advantageous to determine T_e from the portion of the characteristic adjacent to the potential of the isolated probe, using differentiation to eliminate the ion current (see Sec. 4). It is also possible to employ the two-probe method^[29,49,50]. A spherical probe made of a ferromagnet was used in^[51]. A jumplike change in the probe current was observed when the probe temperature passed through the Curie point. These changes were due to a decrease in the tangential component of the magnetic field when the probe went over into the ferromagnetic state.

24. Probe Measurements in the Presence of Directional Motion in the Plasma

In the preceding exposition we assumed an isotropic electron distribution function away from the probe. In real conditions the electrons always have directional motion and current flows through the discharge gap.

This leads to a distortion of the probe characteristics. There is no reliable theory of probe measurements for cases when this distortion is large. When a cylindrical probe is used, this distortion can be avoided if the probe axis is directed along the current. If the axis of the cylindrical probe is perpendicular to the current direction, then the directional motion influences the form of the probe characteristic. A rigorous solution of the problem is impossible, since the potential distribution around the probe does not have cylindrical symmetry.

In^[2] the problem was solved neglecting the asymmetry of the potential. The employed electron distribution relative to the velocity components perpendicular to the probe axis was

$$f_\perp(v_0) = \frac{m}{2\pi k T_e} \exp \left[-\frac{m}{2\pi k T_e} (v_0 - u)^2 \right], \quad (87)$$

with u the drift velocity. Such an analysis can, in our opinion, give only an estimate of the influence of the directional motion at low drift velocities. Calculation has shown that the characteristics remain approximately straight even in the presence of drift, up to $mu^2/2kT_e \sim 0.5$, but the temperature T_e determined from the slope will be exaggerated.

In the case of a spherical probe, if we neglect the asymmetry of the potential, the electron current in a probe situated in a retarding field depends only on the electron energy distribution. The directional motion influences the probe characteristic only via the energy distribution. It is stated on this basis in^[11] that it is possible to employ Eq. (4) in the presence of directional motion. However, the unavoidable asymmetry of the potential makes this statement doubtful. An asymmetry of the field was observed experimentally in^[52].

The directional velocity was measured many times with a unilateral plane probe^[53-56], that is, a probe with one side covered (for example, with mica). The initial premise is that the probe, which is at the space potential, receives all the particles which move in the direction towards the open surface. Then the difference in the current densities (when the probe faces the cathode and then the anode) is equal to the density of the directional current in the discharge $j_0 = n_0 u e$. The concentration n_0 can be determined from the characteristic of the probe when it is turned parallel to the discharge axis.

A compensation circuit for the determination of the current difference, which is usually small, is proposed in^[56]. The idea of the method is to keep the probe in one position and to measure the current difference arising when the probe is rotated.

The described methods of determining the rate of electron drift with the aid of a plane probe appear ineffective to us for the following reasons: The main assumption that when the probe is at the space potential the field surrounding it is equal to zero is not correct in the presence of electron drift relative to the

ions. In fact, let us assume that the field is equal to zero and the particles move freely. We can show that this leads us to a contradiction. The concentrations of the electrons and the ions moving away from the probe to one side are unequal. For example, the concentration of the electrons moving in the electron-drift direction exceeds the concentration of the ions moving in the same direction by an amount $\sim n_0 u / \bar{v}_e$, where \bar{v}_e is the thermal velocity of the electrons. For the opposite direction the inverse holds true, thus ensuring quasineutrality in the unperturbed region. However, near the probe, where the screening is appreciable, quasineutrality is violated. If, for example, the probe faces the cathode, then the electron concentration near the probe will exceed the ion concentration, since there are no particles to move in a direction opposite that of the electron drift. A layer of negative space charge with density $n_0 e u / \bar{v}_e$ will be produced adjacent to the probe and will have a thickness on the order of the probe dimensions. Inside this layer there will be a potential minimum of magnitude $\sim -n_0 e a^2 u / \bar{v}_e$, where a is the probe dimension. For $a = 0.5$ cm and $n_0 = 10^{10}$, the minimum of the potential in volts will be $300 u / \bar{v}_e$. Thus, a deep potential minimum is produced even in the case of a small drift, thus contradicting the initial assumption that the particles move freely. In fact, the produced minimum will be smaller, since the particles do not move freely and tend to neutralize the space charge. However, the potential minimum remains and reflects some of the electrons from the probe. The assumption of free motion of particles around a probe at the space potential is apparently incorrect. If the probe is at the plasma potential and faces the cathode, its current will be smaller than that calculated assuming free motion. The methods described above should therefore yield undervalued drift velocities.

It is indicated in [57] that in the main it is possible to determine the directed part of the electron distribution function from the dependence of the difference of currents obtained for two opposite probe positions on their potential relative to the plasma. This method is analogous to the Druyvestein method for the isotropic part of the distribution and calls for differentiation of the current difference with respect to the probe potential. This method was used experimentally in [58].

A plane probe was also used to study an electron beam in which the random velocity was smaller than the directional velocity [53, 55]. Such conditions obtain in the cathode part of a discharge, where the fast electrons moving from the cathode have not yet acquired a directional velocity. The density of electron current in a flat probe facing the cathode will be

$$j_e = e \int_0^{\infty} n_0 v_z f(v_z) dv_z,$$

where the z axis is perpendicular to the probe on the

probe side, $f(v_z)$ is the distribution of the electrons with respect to the v_z component, and n_0 is the concentration of the beam far away from the probe. If we assume for the distribution function the approximation

$$f(v_z) = \left(\frac{m}{2\pi k T_e} \right)^{1/2} \exp \left[- \frac{m(v_z - u)^2}{2k T_e} \right],$$

then

$$j_e = e n_0 \sqrt{\frac{k T_e}{2\pi m}} e^{-x_m^2} + \frac{e}{2} n_0 u [1 + \Phi(x_m)], \quad (88)$$

where

$$\Phi(x_m) = \frac{2}{\sqrt{\pi}} \int_0^{x_m} e^{-x^2} dx$$

is the probability integral, and

$$x_m = \sqrt{\frac{m}{2k T_e}} \left(u - \sqrt{\frac{2eV}{m}} \right).$$

If the drift velocity is much larger than the thermal velocity, we can neglect the first term of (88), which becomes

$$\Phi(x_m) = \frac{2j_e}{j_0} - 1,$$

where $j_0 = e n_0 u$ is the current density in the beam.

The value of j_0 can be determined from saturation at low negative probe potentials. The quantity $\Phi^{-1}(2j_e/j_0 - 1)$ [Φ^{-1} is the inverse of $\Phi(x)$] should thus be a linear function of the square root of the probe potential. From the slope of the resultant line we can determine the temperature in the beam. In [55] this method was used to investigate an electron beam from an incandescent filament placed in a discharge. At large distances from the filament, good straight lines were observed and the temperature obtained from them corresponded to the filament temperature.

Let us stop in conclusion to discuss the case when the plasma moves as a whole relative to the probe. This occurs when a probe-bearing rocket moves in the ionosphere, or in probe measurements of a plasma jet under laboratory conditions. In [59] there is an approximate calculation of the ion current in a spherical probe which is at a negative potential and moves in the ionosphere, with a rough account of the deformation of the ion sheath around the probe. The calculations were used to find the dependence of the ion concentration on the altitude from rocket measurement data.

V. IMPROVEMENT OF PROBE MEASUREMENT TECHNIQUES AND ERRORS OF THE METHOD

25. Determination of the Space Potential

In order to determine more precisely the space potential in the cases when the point of inflection on the characteristic is not sufficiently pronounced (see Sec. 3), several other methods were proposed.

In [60, 61] variation of the first derivative of the probe current with respect to the potential was used, since

the derivative has a more pronounced variation on going through the space potential than the current itself. The space potential is then taken to be the place where the first derivative has a maximum. The second derivative of the probe current with respect to the potential is even more sensitive^[41,62]; this derivative reverses sign near a probe potential equal to the space potential. It is advantageous to use for the space potential the point of the maximum of the second derivative^[62] (Fig. 20).

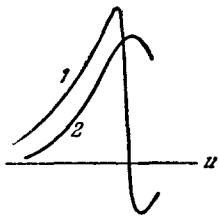


FIG. 20. Variation of the first and second derivatives (2 and 1, respectively) of the probe current near the space potential.

A method proposed in^[63] is based on measuring the noise amplitude in the probe circuit. The maximum of the noise amplitude is observed at a probe potential equal to the space potential. This, however, does not agree with the data of^[64].

Another method is based^[3] on the use of a hot probe. The probe was made in the form of a wire which could be made incandescent by an external voltage source and raised to a temperature corresponding to noticeable electron emission. The characteristics were plotted with the probe both cold and hot. The parts of these characteristics corresponding to a probe positive relative to the plasma coincided, since the potential difference between the probe and the plasma blocked the emission. At negative probe potentials, the current in the hot probe was smaller than in the cold one, owing to the presence of emission from the hot probe. The space potential was taken to be the potential at which the divergence of the characteristics began.

26. Oscillographic Methods of Plotting Probe Characteristics

The general oscillographic measurement scheme consists in the following (Fig. 21). An alternating potential difference is applied between the probe and one of the electrodes (if one probe is used) or between the

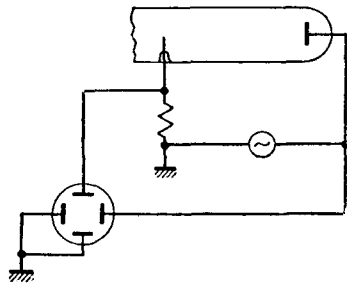


FIG. 21. Simplest diagram for oscillographic measurements.

two probes (in the two-probe method) and is fed through an amplifier to the horizontal deflecting plates of an oscilloscope. (In the case of one probe, a dc bias is introduced to cancel approximately for the potential difference between the plasma at the probe and the electrode.)

A small ohmic resistance is connected in the probe circuit. The voltage drop on this resistance, which is proportional to the probe current, is applied through an amplifier to the vertical plates of the oscilloscope. The characteristic is obtained on the oscilloscope screen in the usual scale, regardless of the wave form of the ac potential difference.

This general circuit is used with various modifications in the following cases.

1. Discharges in which the parameters do not change with time. This includes a dc discharge and a high frequency discharge for which the period is smaller than the relaxation time.

In this case the purpose of using the oscillographic procedure is to reduce the time consumed in the measurement process. Both the simplest variant of the single-probe scheme^[66] and its obvious improvement consisting of making the amplifier for the vertical deflecting plates logarithmic^[67] were used many times for dc discharges. It is possible to display on the oscilloscope screen the entire electron part of the characteristic in a semilog scale. A semiconductor diode, the voltage drop on which is linear with the logarithm of the flowing current, in a wide range, can also be used for this purpose. Such a diode is introduced into the circuit in place of the small ohmic resistance^[68].

At large current densities, to prevent heating the probe, it is advisable to apply the voltage between the probe and the electrode from a pulse generator with low duty cycle^[69].

2. Discharges with periodically varying parameters. These include both discharges with periods larger than the relaxation time and discharges under pulsed conditions and in the deionization mode.

It is of interest in these cases to study the plasma parameters as functions of the phase of the discharge. There are two possible measurements in principle. In the first oscillograms are taken of the probe current with the probe potential fixed for all discharge phases. The points pertaining to the same phase are chosen from the family of probe-current oscillograms plotted at different potentials and the probe characteristic plotted for this phase^[20,57,65]. An analogous method is used for the two-probe circuit in a pulsed discharge^[29,50].

In the second case a definite discharge phase is singled out. If the periodic potential difference in the probe circuit is not synchronized with the period of the discharge, then the probe characteristic for the given phase is obtained on the oscilloscope screen. To single out a definite phase of the discharge it is possible, for example, to cut off the oscilloscope gun by means of a

large negative potential during the entire period with the exception of short time intervals corresponding to the given phase^[10].

We note that in the case of periodic discharges which we are considering it is also possible to dispense with the oscilloscope, by connecting in the probe circuit a switching device which closes the circuit at a definite discharge phase. The characteristic is then plotted point by point^[57].

3. Discharges with aperiodically varying parameters. These include irregular pulsed discharges and various cases when it becomes necessary to deal with a nonstationary plasma. In these cases the oscillographic method is the only one possible, for otherwise one would have to plot the entire characteristic within a time interval during which the parameters of the plasma do not change noticeably. The method has been employed for a powerful pulsed discharge to obtain oscillograms of the characteristic^[17,50] and for rapid plotting of the characteristics in a dc discharge^[71]. The limitations on the rate at which the characteristic is plotted are considered at the end of the present section.

In addition to the oscillographic method described above, different modifications were proposed, in which alternating potential differences with special waveforms were applied to the probe. In one of the methods^[72] the ac potential difference between the probe and one of the electrodes has a sawtooth form so that during one half cycle we have $U = pt$. The vertical plates of the oscilloscope, as in the preceding case, are connected to a small ohmic resistance in series with the probe circuit. The deflection of the beam in the vertical direction is then given by

$$y = Y_0 e^{-\frac{ep}{kT_e} t}$$

for the electron part of the characteristic in the case of a Maxwellian distribution. The voltage applied to the horizontal deflection plates is from a special generator synchronized with the sawtooth generator, and decreases exponentially during the half cycle. Then the horizontal deflection follows the law

$$x = X_0 e^{-t/\tau}$$

By choosing τ it is possible to obtain a linear plot on the oscilloscope screen. Then $kT_e = ep\tau$. By increasing the amplitude of the sawtooth voltage it is possible to obtain a value above which rectification becomes impossible. This enables us to determine the space potential.

Another method^[73] is based on a relation which follows from (5):

$$-\frac{e}{kT_e} = \frac{d}{dV} \log i_e = \frac{1}{i_e} \frac{di_e}{dV} = \frac{1}{i_e} \frac{di_e}{dt} \bigg/ \frac{dV}{dt}$$

If the potential between the probe and the electrode varies linearly in time and if the voltage drop across a small resistance, proportional to i_e , is applied to

one pair of oscilloscope plates and the derivative of this voltage drop is applied to the second pair, then the slope of the obtained line determines T_e . The space potential is determined as the location of the sharp decrease in di_e/dt .

We note in conclusion that there are many factors which limit the rate with which the characteristic can be plotted. First, in the case of rapid variation of the probe potential, the ion layer may not have time to be formed. The time of formation of the layer is on the order of the ratio of the thickness of the plasma region perturbed by the probe to the ion velocity. This condition is not stringent, since this time is usually of the order of microseconds.

Another more serious limitation is connected with the presence of parasitic capacitances in the measuring circuit (Fig. 22). The presence of such capacitances causes parasitic currents of the order of CV/τ (where τ is the time necessary to plot one characteristic) to appear in the probe circuit. In order for this measurement to be possible, the probe current must exceed the parasitic current. For example, if $C = 10$ pF, $V = 100$ V, and $\tau = 1$ μ sec, the parasitic current is ~ 1 mA.

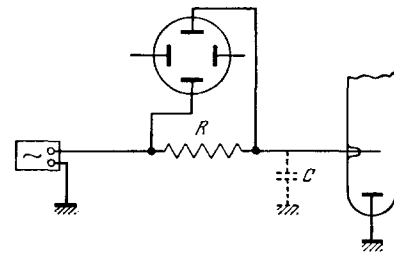


FIG. 22. Parasitic capacitances in oscillograph circuit.

27. Methods of Differentiating the Probe Characteristic

In many cases it is necessary to determine the first or second derivative of the probe current with respect to the probe potential. This is necessary in order to exclude the ion current (see Fig. 4) and to find the electron velocity distribution [see (4)].

1. Methods of graphic differentiation. The simplest method is to divide the interval of the potentials into small sections ΔV and replace the derivative by the quantity $\Delta i/\Delta V$. This procedure was carried out twice by Druyvestein^[12] to find the energy distribution of the electrons in the positive column in neon. A certain modification of this procedure was used in^[74]. A single differentiation was used to find the electron temperature T_e by determining the start of the electronic part of the characteristic^[8,75]. This method is generally speaking not very accurate, while in the case of double differentiation the errors increase greatly and only qualitative results can be expected.

Some modification of the graphic method of double

differentiation^[76] is to plot the characteristic in a semilogarithmic scale (in which it is smoother) and use the relation

$$\frac{1}{i} \frac{d^2 i}{dV^2} = \left(\frac{d}{dV} \ln i \right)^2 + \frac{d^2}{dV^2} \ln i.$$

This analysis method was used to find the energy distribution of the electrons in a glow discharge.

2. Method of superposition of an alternating potential. In addition to the constant potential difference there is connected in the probe circuit an ac sinusoidal potential generator $u_1 = A \cos \omega t$ (Fig. 23). The potential is then $u + u_1$, and the current

$$i = f(u + A \cos \omega t).$$

If the amplitude A is sufficiently small, then

$$\begin{aligned} i &= f(u) + f'(u) A \cos \omega t + \frac{1}{2} f''(u) A^2 \cos^2 \omega t + \dots \\ &= \left[f(u) + \frac{1}{4} A^2 f''(u) + \dots \right] + [A f'(u) + \dots] \cos \omega t + \dots \end{aligned}$$

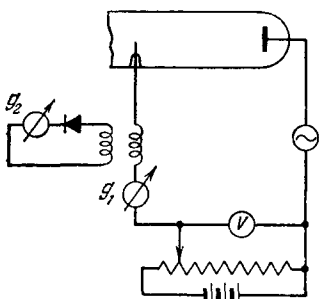


FIG. 23. Simplest circuit for measuring the derivatives of the probe current by superposition of an alternating potential.

We see therefore that by measuring the ac component of the current at the frequency ω in the probe circuit it is possible to determine the first derivative of the probe current $f'(u)$. By measuring the addition to the dc component, resulting from turning on the ac voltage, we can determine the second derivative of the probe current $f''(u)$. By varying the potential difference u with the aid of a potentiometer, we obtain the first or second derivative of the current in the required portion of the characteristic.

To measure the first derivative we can, for example, connect in the probe circuit a small inductance^[60], which serves as the primary winding of a step-up transformer. The amplitude of the ac potential difference produced in the secondary winding can be observed on the oscilloscope screen or with a galvanometer connected in the circuit in place of the oscilloscope, in series with a rectifier unit. This method can lead to errors if considerable oscillations are present in the plasma. To reduce these errors, a judicious choice of the frequency ω is necessary, as well as the use of a filter^[61].

To measure the second derivative $f''(u)$ it is necessary to measure the small addition to the dc component of the probe current. To this end a special compensating circuit was used in^[78]. An essential

shortcoming of this method is that it can be used only under exceedingly stable discharge conditions. The method of obtaining the second derivative can be improved by using in place of a sinusoidal potential difference a variable potential difference in the form

$$u_1 = A(1 + \cos \omega_1 t) \sin \omega_2 t,$$

where $\omega_1 \ll \omega_2$. Then

$$\begin{aligned} i &= f(u + u_1) = f(u) + \frac{3}{8} A^2 f''(u) \\ &+ \left[\frac{A^2}{2} f''(u) + \dots \right] \cos \omega_1 t + \Sigma, \end{aligned}$$

where Σ is the sum of the ω_2 components that decrease in amplitude and of the multiple and combination frequency components. Thus, in this case $f''(u)$ determines the amplitude of the ac component with frequency ω_1 and facilitates its measurement. The voltage-drop component of frequency ω_1 , produced across a small resistance connected in the probe circuit, is separated with the aid of a narrow band amplifier and applied through a detector to the vertical plates of the oscilloscope. The potential difference u applied to the horizontal deflecting plates comes from a generator that produces a slowly varying potential difference and is connected between the probe and the electrode. This made it possible to produce rapidly (within 25 seconds) the entire $f''(u)$ curve on the oscilloscope screen. This method was used to investigate the electron energy distribution in a mercury discharge in the presence of striations^[79]. A similar method is described in^[41], where the errors of procedures of this type are also discussed. We note that it is also possible to measure the amplitude of the harmonic ω_1 directly, with a vacuum tube voltmeter connected past the narrow band amplifier. The $f''(u)$ curve is plotted in this case point by point.

3. Use of differentiating networks. In this method the potential of the probe relative to the anode is varied by applying a voltage from a sawtooth generator, which produces a linear dependence of the voltage on the time. The voltage drop on a small resistance in the probe circuit is proportional to the probe current and is applied to the vertical deflecting plates of the oscilloscope. The voltage applied to the horizontal plates is from a sawtooth generator. In view of the proportionality between the probe sawtooth voltage to the time, the oscilloscope screen displays the dependence of the derivative of the probe current with respect to the probe potential as a function of the probe potential. The method is used to obtain both the first^[80] and the second derivative^[81]. This method can be used in cases when the conditions in the plasma vary rapidly.

28. Some Other Probe Applications

Let us dwell briefly on some additional possibilities of the use of probes.

Two probes placed in different points of the plasma can be used to measure the potential difference between these points. To this end it would be necessary to determine the space potential for each of the probes and take their difference. If the probes as well as the properties of the plasma at the locations of the probes are identical, then it is possible to use simply the difference between the potentials of the floating probes. The latter is determined as the potential difference between the two probes when the current in the two-probe circuit is equal to zero. If the properties of the plasma at the probe locations are not the same, then this method results in an error of the order of kT_e/e .

With the aid of a wall probe it is possible to measure the flux of charged particles at the wall of a discharge tube. To this end we use the fact that the ion current depends little on the probe potential, and extrapolate the current from large negative probe potentials to the wall potential (usually the current at the wall is zero and consequently the wall potential corresponds to the floating potential of the probe).

Different methods for determining the gas density with the aid of probes were proposed in [82,83]. An attempt was made in [84] to determine the plasma parameters by measuring the energy flux to the probe at different probe potentials.

Attempts were made frequently to determine the ion temperature T_p from the ion part of the characteristic. All these attempts were based on the old Langmuir ion-current theory and are therefore inconsistent. As can be seen from the results of Ch. II, the ion current is practically independent of the ion temperature at large negative probe potentials, so that determination of T_p by the probe method is practically impossible. To determine T_p it is possible to use the method of retarding field [5,85] and spectrochemical methods [86,87].

High frequency methods were recently developed for plasma research. The probes are used here as miniature oscillating systems. The properties of such a system depend on the dielectric constant of the plasma in which it is immersed, and make it possible to determine the electron concentration [88].

In many investigations the probe was used to study the spectrum of plasma noise [89]. The electron temperature can be determined from the intensity of the noise in the microwave band [90].

29. Sources of Errors in Probe Measurements

In order that the probe measurements yield correct results, the conditions under which the probe operates must correspond to the theoretical scheme considered above. Under real conditions there are many external factors which can distort the results of the probe measurements and make their interpretation difficult. Let us consider in succession the influence of these factors.

1. Contamination of the probe surface. Contaminations may change the work function of the probe or

form surface layers with large ohmic resistances. If the probe electron current is small and the probe is cold, a deposit is formed on the probe. With increasing electron current in the probe, when the latter becomes heated, or in the case of large negative probe potentials when ion bombardment becomes appreciable, the contaminations are evaporated from the surface. The probe characteristic can be made perfectly reproducible if it is measured sufficiently slowly, but nonetheless the characteristic will be deformed. The point is that the variation of the probe potential registered by the voltmeter will differ from the variation of the potential at the surface of the probe, if the work function or the potential drop on the surface layer changes at the same time. In addition, variations of the surface conditions change the electron reflection coefficient [14]. All these factors influence essentially the part of the characteristic which corresponds to low negative probe potentials and is used to determine the temperature of the electron gas or the velocity distribution of the electrons. Some influence of contamination by mercury was observed in [91,92]. The characteristic becomes strongly distorted if the probe becomes contaminated with vapor of the lubricant [90] or of barium oxide (when working with oxide cathodes). To prevent this distortion it is necessary to clean the probe by electron or ion bombardment before the measurements, and to perform the measurements quite rapidly. A pulse circuit which combines continuous cleaning of the probe with rapid plotting of the characteristic is proposed in [71,111].

2. Probe dimensions and insulation. The dimensions of the probe in a positive column are limited by many circumstances. Too large a probe introduces essentially geometric distortion in the discharge gap. In addition, the electric distortion connected with the distribution of the current in the discharge circuit and in the probe circuit is significant. Changes of this kind are caused by distortions in the region of the probe characteristic near the space potential [94,95]. However, even if the ion part of the probe characteristic is used and the probe current is much smaller, the probe must still be sufficiently small [10].

The plasma region perturbed by the probe has dimensions on the order of the impact parameter p_0 at which the ion strikes the probe. The theory proposed above for the ion part of the probe characteristic neglects ionization in this region. It can be assumed for estimating purposes that all the ions produced in this region as a result of ionization reach the probe. The current due to these ions is zn_0V , where z is the number of ionizations per electron and V is the volume of the perturbed region. z can be estimated from the balance condition of the positive column [96]. If the mean free path λ of the ion is much larger than the tube radius R , then

$$z \cong 0.8 \sqrt{\frac{2kT_e}{M}} \frac{1}{R}.$$

In the opposite case

$$z = (2.4)^2 \frac{D_a}{R^2} \cong 2 \sqrt{\frac{2kT_e}{M}} \sqrt{\frac{T_e}{T}} \frac{\lambda}{R^2}$$

(when $T_e \gg T$). The condition that the probe current due to ionization in the perturbed region be small compared with the current that goes to the probe from the unperturbed plasma [formulas (35) and (52)], leads to the following limitations of the probe dimensions (when $T_e \gg T$). In the case of low pressures ($\lambda \gg R$)

$$r_s \ll \left(\frac{T}{T_e}\right)^{3/4} R$$

for a spherical probe and

$$r_s \ll \frac{T}{T_e} R$$

for a cylindrical probe. At high pressures ($\lambda \ll R$)

$$r_s \ll 0.2 \frac{R}{\lambda} \left(\frac{T}{T_e}\right)^{5/4} R$$

for a spherical probe and

$$r_s \ll 0.2 \frac{R}{\lambda} \left(\frac{T}{T_e}\right)^{3/2} R$$

for a cylindrical probe. The sheath radius r_s can be assumed to be equal to the radius of the probe in the estimates.

Another limitation on the probe dimensions is connected with neglecting the collisions in the unperturbed region. For the ion current (when $T_e \gg T$) this is legitimate if $p_0 \ll \lambda$, that is,

$$r_s \ll \lambda \left(\frac{T}{T_e}\right)^{1/2}$$

for a cylindrical probe and

$$r_s \ll \lambda \left(\frac{T}{T_e}\right)^{1/4}$$

for a spherical probe. For the electron part of the characteristic, collisions can be neglected if the probe dimension is much smaller than the mean free path of the electron [3,97].

It is pointed out in [11] that ions can have closed orbits in the attracting field of the probe. The ion may go into such an orbit only as a result of collisions. However, the population of these orbits will not depend on the collision frequency, since the ion can leave the orbit only as a result of collisions. The authors give for the ratio of the probe radius to the Debye radius, a lower limit at which there are still no closed orbits. If the radius of the probe is smaller than that determined by this criterion, then the "captured" ions may influence the distribution of the charge and of the potential. An account of this influence is very difficult, but it seems to us that it is small under ordinary discharge conditions. In order for the ion to go into a closed orbit, its centrifugal force must become equal to the attraction force. Yet after collision with neu-

tral atoms (charge exchange) the ions become thermal. Therefore a very small fraction of the collisions can cause an ion to go into a closed orbit, whereas any collision can take the ion out of the orbit.

The non-working part of the probe is protected with an insulator, which becomes charged negatively in the discharge and is surrounded by a layer of positive space charge. The latter decreases the effective surface of the probe, and this can lead to errors in the determination of the concentration n_0 . An attempt to study this effect was made in [98]. In [95] it is indicated that the characteristics of a plane probe becomes distorted near the wall, owing to the influence of the space-charge layer at the wall. In the same investigation, a study was made of the probe characteristics for several cylindrical and spherical probes of different lengths and diameters, and with different thickness of the insulating surface. On the basis of such a comparison, the author has reached the conclusion that the most suitable for measurements are thin cylindrical probes with long non-insulated surfaces and thin insulation. When a short cylindrical probe is used, an error may arise as a result of failure to take into account the current in the end section of the layer. This question is considered in [99].

3. Effect of oscillations of the plasma potential on the probe characteristic. Oscillations of the plasma potential in the vicinity of the probe can greatly deform the electron and the start of the ion part of the characteristic. If the frequency of these oscillations is not too high, so that the electron current can reach steady state within one period (within approximately the time of passage of the electron through the perturbed region), then the instrument averages the current. The strong nonlinearity of the probe characteristic causes distortion (Fig. 24) [3].

As can be seen from Fig. 24, the temperature T_e will be overestimated. The influence of the oscillations on the probe current was observed in [50,95,100] and methods were proposed to suppress the oscillations. The question of the influence of oscillations on the characteristic is also discussed in [110].

4. Effect of an electron emission from the probe. The emission may be due to impact by positive ions, metastable atoms, and photons. This leads to an overestimate of the ion current at negative probe potentials. In order to estimate the emission due to positive ions,

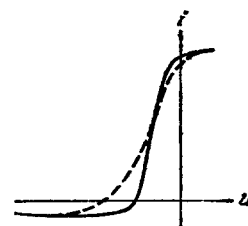


FIG. 24. Influence of oscillations on the probe characteristic. The dashed line shows the distorted characteristic.

it is necessary to know the coefficient of secondary emission from the probe material for ions with energy corresponding to the negative potential of the probe. For energies lower than 100 V, the emission coefficient is of the order of 10^{-1} – 10^{-2} ^[57]. It must be borne in mind that contamination of the probe surface may increase the emission coefficient.

Emission under the influence of metastable atoms and photons was investigated in many studies^[101,102,5]. This effect should be most strongly pronounced in inert gases, which have high excitation potentials. In^[5] the value obtained for the ratio of the emission current for a discharge in argon, at pressures 10^{-3} –1 mm Hg and currents 200–100 mA (under the influence of metastable atoms and photons), to the ion current in the probe is from 5 to 20%. To estimate the emission it is necessary to know the concentration of the excited atoms in the discharge. The emission current under the influence of the metastable atoms is given by the expression

$$\frac{en_m \bar{v} S}{4} \gamma_m,$$

where n_m is the concentration of the metastable atoms, \bar{v} their average velocity, S the probe surface area, and γ_m the emission coefficient, which is of the order of 10^{-1} – 10^{-2} ^[57,109]. The emission current under the influence of photons can be estimated from the formula^[103]

$$i_e = \frac{en_a S}{4\tau k_0} \gamma_{ph},$$

where n_a — concentration of the excited atoms, k_0 — absorption coefficient, τ — lifetime of the excited atom, and γ_{ph} — quantum yield. Some data on γ_{ph} are contained in^[57,109]. An example of such an estimate is given in^[104]. At large negative probe potentials (on the order of hundreds of electron volts), intense impact ionization by electrons knocked out from the probe is possible, along with avalanche formation. This is apparently the cause of the sharp increase of the ion current in the probe, observed at these potentials. This section of the characteristic can therefore not be used for the measurement of the plasma parameters.

30. Conclusion

The method of Langmuir probes is reliably based both theoretically and experimentally for the investigation of an isotropic low-pressure plasma in sufficiently weak magnetic fields. Further development of probe procedures must proceed, in our opinion, along the following main lines.

1. Use of probes at pressures when the mean free path of the plasma particles is smaller than the probe dimensions. Attempts to extend the probe theory to this case were made in^[105,106]. In^[104] a method is given for finding the plasma parameters and for the measurement of the parameters in mercury and inert

gases in the pressure interval 1–20 mm Hg. It is desirable to accumulate further experimental material, particularly at high pressures.

2. Probe measurements in the presence of directional motion in the plasma. The material reported in Sec. 24 shows that there is still no satisfactory solution of this problem.

3. Use of probes in the presence of a strong magnetic field. In spite of the importance of this question, there has been no appreciable progress in this direction to date.

4. Not strictly Maxwellian velocity distribution of the electrons. Deviations are particularly significant in the energy region in which inelastic collisions are possible^[107,108]. Particular interest attaches therefore to further improvement of methods for determining the electron distribution function, particularly at high energies.

LIST OF SYMBOLS

- $f_0(v), F_0(v)$ — electron and ion velocity distribution functions in plasma,
- u_0 — plasma potential relative to the anode or cathode (space potential),
- u — potential of probe relative to the anode or cathode,
- $-V(r)$ — potential of a given point in the vicinity of the probe relative to the unperturbed plasma,
- $-V(a) \equiv -V$ — potential of the probe relative to the unperturbed plasma,
- $-V_1$ — potential of isolated (floating) probe relative to the unperturbed plasma,
- $-i_e$ — electron current in probe,
- i_p — ion current in probe,
- i — total current in probe,
- $-i_0$ — electron current in probe at space potential,
- $-j_e$ — density of electron current in probe,
- n_0 — concentration of electrons in plasma,
- $n_e(r), n_p(r)$ — concentration of electrons and ions in the vicinity of the probe,
- T_e, T_p — temperatures of electron and ion gases,
- \bar{v}_e, \bar{v}_p — average velocities of electrons and ions,
- ϵ_0 — quantity on the order of the average ion energy,
- a — probe radius,
- r_p — radius of ion layer,
- r_s — radius of space charge sheath,
- r_l — radius of limitation sphere,
- S — probe area
- $h = (kT_e/4\pi n_0 e^2)^{1/2}$ — Debye radius,
- e — absolute value of electron (ion) charge,
- m, M — masses of electron and ion,
- $x = r/r_l, x_s = r_s/r_l, x_p = r_p/r_l, \gamma = \epsilon_0/kT_e,$
- $\eta = eV(r)/kT_e, \eta_l = eV(r_l)/kT_e, \eta_s =$
- $= eV(r_s)/kT_e, \eta_p = eV(r_p)/kT_e$ — dimensionless quantities.

¹ J. Langmuir and H. Mott-Smith, Gen. Electr. Rev. 27, 449, 538, 616, 762, 810 (1924).

² J. Langmuir and H. Mott-Smith, Phys. Rev. 28, 727 (1926).

- ³The Characteristics of Electrical Discharges in Magnetic Fields, Ed. by A. Guthrie and R. Wakerling, New York, 1949.
- ⁴F. Wenzl, *Z. angew. Phys.* **2**, 59 (1950).
- ⁵R. Boyd, *Proc. Roy. Soc. A201*, 329 (1950).
- ⁶Yu. M. Kagan and V. I. Perel', *DAN SSSR* **91**, 1321 (1953) and **95**, 765 (1954).
- ⁷Yu. M. Kagan and V. I. Perel', *JETP* **29**, 261 (1955), *Soviet Phys. JETP* **2**, 326 (1956); *Trudy, Karelian State University* **4**, 69 (1955).
- ⁸Kagan, Perel', and Ripatti, *Vestnik, Leningrad State University*, No. 8, 129 (1955).
- ⁹Yu. M. Kagan, *ibid.*, No. 4, 63 (1957).
- ¹⁰Allen, Boyd, and Reynolds, *Proc. Phys. Soc.* **70**, 297 (1957).
- ¹¹J. Bernstein and J. Rabinowitz, *Phys. Fluids* **2**, 112 (1959).
- ¹²M. Druyvestein, *Zs. Phys.* **64**, 781 (1930).
- ¹³H. Rothman, *Studii si cercetari de fizica* **8**, 255 (1957); *DAN SSSR* **120**, 999 (1958).
- ¹⁴I. M. Bronshtein, *Izv. AN SSSR ser. fiz.* **22**, 441 (1958), *Columbia Tech. Transl.* p. 442; I. M. Bronshtein and V. V. Roshchin, *ZhTF* **28**, 2200 and 2476 (1958), *Soviet Phys. Tech. Phys.* **3**, 2023 and 2271 (1959).
- ¹⁵G. Nicoll and J. Basu, *J. Electr. and Control* **12**, 23 (1962).
- ¹⁶J. Langmuir and Blodgett, *Phys. Rev.* **22**, 317 (1923); **24**, 49 (1924).
- ¹⁷Brunet, Geller, and Leroy, *Report CEA No. 1580*.
- ¹⁸N. A. Kaptsov, *Elektricheskie yavleniya v gazakh (Electric Phenomena in Gases)*, Gostekhizdat, 1950.
- ¹⁹E. Hayess and K. Rademacher, *Ann. d. Phys.* **8**, 158 (1961).
- ²⁰E. Johnson and L. Malter, *Phys. Rev.* **80**, 59 (1950).
- ²¹L. M. Biberman and B. Panin, *ZhTF* **21**, 2 (1951).
- ²²S. Kojima and K. Takayama, *J. Phys. Soc. Japan* **4**, 346 (1949); **5**, 357 (1950).
- ²³Vagner, Kagan, and Perel', *Vestnik, Leningr. State Univ.* No. 22, 75 (1956).
- ²⁴K. Jamamoto and T. Okuda, *J. Phys. Soc. Japan* **11**, 57 (1956).
- ²⁵S. D. Vagner, *ZhTF* **28**, 2739 (1958), *Soviet Phys. Tech. Phys.* **3**, 2507 (1959).
- ²⁶Kagan, Kal'vinova, and Raudanen, *Vestnik, Leningr. State Univ.* No. 16, 41 (1957).
- ²⁷V. V. Avramov and Kh. A. Dzherpetov, *Vestnik, Moscow State Univ.* No. 3, 55 (1960).
- ²⁸S. M. Levitskiĭ and I. P. Shashurin, *Radiotekhnika i élektronika* **4**, 1238 (1959); R. Knechtli and J. Wada, *Phys. Rev. Lett.* **6**, 215 (1961).
- ²⁹Demirkhanov, Leont'ev, and Kosyĭ, *ZhTF* **32**, 180 (1962), *Soviet Phys. Tech. Phys.* **7**, 125 (1962).
- ³⁰Kh. A. Dzherpetov and G. M. Pateyuk, *JETP* **28**, 343 (1955), *Soviet Phys. JETP* **1**, 326 (1955).
- ³¹T. Okuda and K. Jamamoto, *J. Appl. Phys.* **31**, 158 (1960).
- ³²H. Fetz and H. Öchsner, *Z. angew. Phys.* **12**, 250 (1960).
- ³³Vagner, Zudov, and Khahaev, *ZhTF* **31**, 336 (1961), *Soviet Phys. Tech. Phys.* **6**, 240 (1961).
- ³⁴S. D. Vagner and Ya. F. Verolainen, *Uch. Zap. (Science Notes), Karelian Pedagog. Inst.* **11**, No. 1, 69 (1961).
- ³⁵Kojima, Takayama, and Shimachi, *J. Phys. Soc. Japan* **8**(1), 55 (1953).
- ³⁶S. D. Vagner, *Uch. zap. (Science Notes) Petrozavodsk Univ.* **5**, No. 4, 129 (1957).
- ³⁷Vavilin, Vagner, Lanenkina, and Mitrofanova, *ZhTF* **30**, 1064 (1960), *Soviet Phys. Tech. Phys.* **5**, 996 (1961).
- ³⁸Vavilin, Vagner, and Platonov, *Fiziko-technicheskiĭ sbornik (Physico-technical Collection), Petrozavodsk, in press.*
- ³⁹R. Boyd and J. Thompson, *Proc. Roy. Soc. A252*, 102 (1959).
- ⁴⁰J. Thompson, *Proc. Phys. Soc.* **73**, 818 (1959).
- ⁴¹R. Boyd and N. Twiddy, *Proc. Roy. Soc. A250*, 53 (1959).
- ⁴²N. Twiddy and R. Boyd, *Proc. Roy. Soc. A259*, 145 (1960).
- ⁴³J. Wilhelm, *Ann. d. Phys.* **12**, 401 (1953).
- ⁴⁴J. Spencer-Smith, *Phil. Mag.* **19**, 806 (1935).
- ⁴⁵E. M. Reĭkhrudel' and G. V. Spivak, *JETP* **6**, 816 (1936) and **8**, 319 (1938).
- ⁴⁶B. Bertotty, *Phys. Fluids* **4**, 1047 (1961); I. K. Fetisov, *JETP* **36**, 1110 (1959), *Soviet Phys. JETP* **9**, 789 (1959).
- ⁴⁷L. A. Artsimovich, *Upravlyaemye termoyadernye reaktsii (Controlled Thermonuclear Reactions)*, *Fizmatgiz*, 1961; A. V. Zharinov, *Atomnaya énergiya* **7**, 215 (1959).
- ⁴⁸R. Bickerton and A. von Engle, *Proc. Phys. Soc. B69*, 468 (1956).
- ⁴⁹Vagner, Kagan, and Romanova, *Vestnik, Leningr. State Univ.* No. 10, 15 (1958).
- ⁵⁰V. I. Pistunovich, *Fizika plazmy i problema upravlyaemykh termoyadernykh reaktsii (Plasma Physics and the Problem of Controlled Thermonuclear Reactions)*, v. IV, 1948, p. 134; J. Jones and P. Sanders, *J. Sci. Instr.* **37**, 457 (1960).
- ⁵¹M. D. Gabovich, *Trudy, Phys. Inst. Acad. Sci.* No. 7, 44 (1956).
- ⁵²T. Okuda and J. Jamamoto, *J. Phys. Soc. Japan* **13**, 1212 (1958).
- ⁵³S. D. Gvozdover, *ZhTF* **3**, 587 (1933).
- ⁵⁴Rozhanskiĭ, Kovalenko, and Sena, *ZhTF* **4**, 1271 (1934).
- ⁵⁵V. Polin and S. D. Gvozdover, *JETP* **8**, 436 (1938).
- ⁵⁶Fataliev, Spivak, and Reĭkhrudel', *JETP* **9**, 167 (1939).
- ⁵⁷V. L. Granovskiĭ, *Elektricheskiĭ tok v gaze (Electric Current in Gases)* v. 1, Gostekhizdat, 1952.
- ⁵⁸G. D. Lobov and V. V. Zakharov, *Radiotekhnika i élektronika* **7**, 652 (1962).

- ⁵⁹ Dote, Takayama, and Jchumiya, *J. Phys. Soc. Japan* **17**, 174 (1962).
- ⁶⁰ Yu. M. Kulakov and A. A. Zaitsev, *Vestnik, Moscow State Univ. No. 3*, 101 (1949).
- ⁶¹ F. Nölle, *Ann. d. Phys.* **18**, 328 (1956).
- ⁶² Vorob'eva, Kagan, and Melenin, *ZhTF* **33**, 571 (1963), *Soviet Phys. Tech. Phys.* **8**, 423 (1963).
- ⁶³ Zaitsev, Vasil'eva, and Mnev, *JETP* **36**, 1590 (1959), *Soviet Phys. JETP* **9**, 1130 (1959).
- ⁶⁴ R. Sears and J. Brophy, *Bull. Amer. Phys. Soc.*, No. 6, 413 (1960).
- ⁶⁵ V. L. Granovskii, *Izv. AN SSSR No. 4*, 449 (1938).
- ⁶⁶ See, e.g., F. Anderson, *Phil. Mag.* **38**, 179 (1947).
- ⁶⁷ Johnston, *Brit. J. Appl. Phys.* **7**, 266 (1956).
- ⁶⁸ S. M. Levitskii and Z. A. Plyatsok, *PTE*, No. 2, 150 (1961).
- ⁶⁹ B. A. Mamyurin, *ZhTF* **23**, 904 and 1915 (1953).
- ⁷⁰ R. Ledrus, *Appl. Sci. Res.* **B5**, No. 1-4, 151 (1955).
- ⁷¹ J. Waymouth, *J. Appl. Phys.* **30**, 1404 (1959).
- ⁷² A. M. Bonch-Bruevich, *DAN SSSR* **81**, 371 (1951).
- ⁷³ H. Tamagawa and J. Tujita, *J. Phys. Soc. Japan* **14**, 678 (1959).
- ⁷⁴ G. Medicus, *J. Appl. Phys.* **27**, 10 (1956).
- ⁷⁵ V. M. Zakharova and Yu. M. Kagan, *Optika i spektroskopiya* **1**, 627 (1956).
- ⁷⁶ R. Sloane and K. Emeleus, *Phys. Rev.* **44**, No. 5, (1933).
- ⁷⁷ K. Emeleus and R. Ballantine, *Phys. Rev.* **50**, 672 (1936).
- ⁷⁸ R. Sloane and E. McGregor, *Phil. Mag.* **18**, 193 (1934).
- ⁷⁹ G. M. Malyshev and V. L. Fedorov, *DAN SSSR* **92**, 259 (1953).
- ⁸⁰ Kagan, Malyshev, and Fedorov, *ZhTF* **23**, 894 (1953); *B. Smithers, J. Sci. Instr.* **39** (1), 21 (1962).
- ⁸¹ Kagan, Fedorov, Malyshev, and Gavallas, *DAN SSSR* **76**, 215 (1951).
- ⁸² Klyarfel'd, Timofeev, Neretina, and Guseva, *ZhTF* **25**, 1580 (1955).
- ⁸³ Rubchinskiĭ, Kobelev, and Mantrov, *Radiotekhnika i elektronika* **4**, 1311 (1959).
- ⁸⁴ M. M. Gorshkov and Yu. P. Maslakovets, *ZhTF* **6**, 1513 (1936).
- ⁸⁵ N. I. Ionov, *DAN SSSR* **85**, 753 (1952).
- ⁸⁶ S. É. Frish and Yu. M. Kagan, *ZhTF* **18**, 519 (1948).
- ⁸⁷ Zaidel', Malyshev, and Shreĭder, *ZhTF* **31**, 129 (1961), *Soviet Phys. Tech. Phys.* **6**, 93 (1961).
- ⁸⁸ S. M. Levitskii and I. P. Shashurin, *Izv. AN SSSR* **23**, 948 (1959), *Columbia Tech. Transl.* p. 938; *ZhTF* **31**, 436 (1961), *Soviet Phys. Tech. Phys.* **6**, 315 (1961). Takayama, Ikegami, Miyazaki, *Phys. Rev. Lett.* **5**, 238 (1960).
- ⁸⁹ G. Singh, *Proc. Phys. Soc.* **74**, 42 (1959); A. Galbraith and A. van der Ziel, *Proc. of the Fourth Intern. Conf. on Ioniz. Phenomena in Gases*, vol. I, Amsterdam, 1960; K. Emeleus, *Plasma Physics* **2**, 65 (1961).
- ⁹⁰ K. Knol, *Philips Res. Repts.* **6**, 288 (1951); M. Easley and W. Mumford, *J. Appl. Phys.* **22**, 846 (1951).
- ⁹¹ R. Howe, *J. Appl. Phys.* **24**, 7 (1953).
- ⁹² M. Easley, *J. Appl. Phys.* **22**, 590 (1951).
- ⁹³ G. Wehner and G. Medicus, *J. Appl. Phys.* **23**, 1035 (1952).
- ⁹⁴ B. N. Klyarfel'd, *Trudy, All-union Electrotechnical Institute*, No. 41, 162 (1940).
- ⁹⁵ L. G. Guseva, *ZhTF* **21**, 426 (1951).
- ⁹⁶ W. Schottky, *Phys. Zs.* **25**, 342 (1924); *J. Langmuir and L. Tonks, Phys. Rev.* **24**, 876 (1929).
- ⁹⁷ Yu. M. Kagan and V. I. Perel', *ZhTF* **24**, 889 (1954).
- ⁹⁸ M. Fiebich, *Acta Physica Austriaca* **4**, 170 (1950).
- ⁹⁹ T. Okuda and K. Jamamoto, *J. Phys. Soc. Japan* **13**, 411 (1958).
- ¹⁰⁰ L. A. Sena, *JETP* **16**, 811 (1946).
- ¹⁰¹ W. Uyterhoven and M. Harrington, *Phys. Rev.* **36**, 709 (1930); *Kenty, Phys. Rev.* **43**, 181 (1933).
- ¹⁰² G. V. Spivak and E. M. Reĭkhrudel', *ZhTF* **3**, 983 (1933).
- ¹⁰³ V. A. Fabrikant, *JETP* **17**, 1037 (1947).
- ¹⁰⁴ Zakharova, Kagan, Mustafin, and Perel', *ZhTF* **30**, 442 (1960), *Soviet Phys. Tech. Phys.* **5**, 411 (1960).
- ¹⁰⁵ B. I. Davydov and L. I. Zmanovskaya, *ZhTF* **6**, 1244 (1936).
- ¹⁰⁶ R. Boyd, *Proc. Phys. Soc.* **B64**, 795 (1951).
- ¹⁰⁷ Yu. M. Kagan and R. I. Lyagushchenko, *ZhTF* **31**, 445 (1961) and **32**, 192 (1962), *Soviet Phys. Tech. Phys.* **6**, 321 (1961) and **7**, 134 (1962).
- ¹⁰⁸ Yu. M. Kagan and R. I. Lyagushchenko, *ZhTF* **32**, 735 (1962), *Soviet Phys. Tech. Phys.* **7**, 535 (1962).
- ¹⁰⁹ J. Hasted, *J. Appl. Phys.* **30**, 22 (1959).
- ¹¹⁰ K. Emeleus, *Plasma Physics* **2**, 69 (1961).
- ¹¹¹ B. Richelman, *Rev. Sci. Instr.* **30**, 593 (1959).
- ¹¹² D. Kamke and H. Rose, *Zs. Phys.* **145**, 83 (1956).

Translated by J. G. Adashko